

Journal of Visualized Experiments

An affordable and efficient “homemade” platform for *Drosophila* behavioral studies, and an accompanying protocol for larval mitochondrial respirometry
--Manuscript Draft--

Article Type:	Invited Methods Collection - Author Produced Video
Manuscript Number:	JoVE62669R1
Full Title:	An affordable and efficient “homemade” platform for <i>Drosophila</i> behavioral studies, and an accompanying protocol for larval mitochondrial respirometry
Corresponding Author:	Marcos T Oliveira, Ph.D. Universidade Estadual Paulista Julio de Mesquita Filho Jaboticabal, SP BRAZIL
Corresponding Author's Institution:	Universidade Estadual Paulista Julio de Mesquita Filho
Corresponding Author E-Mail:	marcos.t.oliveira@unesp.br
Order of Authors:	Geovana Garcia Murilo Othonicar Marcos T Oliveira, Ph.D. Carlos Couto-Lima
Additional Information:	
Question	Response
Please specify the section of the submitted manuscript.	Behavior
Please indicate whether this article will be Standard Access or Open Access.	Standard Access (\$1400)
Please confirm that you have read and agree to the terms and conditions of the author license agreement that applies below:	I agree to the Author License Agreement
Please provide any comments to the journal here.	
Please confirm that you have read and agree to the terms and conditions of the video release that applies below:	I agree to the Video Release

TITLE:

An affordable and efficient “homemade” platform for *Drosophila* behavioral studies, and an accompanying protocol for larval mitochondrial respirometry

AUTHORS AND AFFILIATIONS:

Geovana S. Garcia¹, Murilo F. Othonicar², Marcos T. Oliveira^{3,*,#}, Carlos A. Couto-Lima^{4,*}

¹Departamento de Tecnologia, Faculdade de Ciências Agrárias e Veterinárias, Universidade Estadual Paulista “Júlio de Mesquita Filho”, Jaboticabal, SP, Brazil, geovana.garcia@unesp.br

²Departamento de Tecnologia, Faculdade de Ciências Agrárias e Veterinárias, Universidade Estadual Paulista “Júlio de Mesquita Filho”, Jaboticabal, SP, Brazil, murilo.othonicar@unesp.br

³Departamento de Tecnologia, Faculdade de Ciências Agrárias e Veterinárias, Universidade Estadual Paulista “Júlio de Mesquita Filho”, Jaboticabal, SP, Brazil, marcos.t.oliveira@unesp.br

⁴Faculdade de Ciências da Saúde, Biomedicina, Universidade do Oeste Paulista, Presidente Prudente, SP, Brazil, carloscouto@unoeste.br

*shared senior authorship

#corresponding author

SUMMARY:

We provide protocols for anyone with a “maker culture” mind to start building a flylab for quantitative analysis of a myriad of behavioral parameters in *Drosophila melanogaster*, by 3D-printing many of the necessary pieces of equipment. We also describe a high resolution respirometry protocol using larvae to combine behavioral and mitochondrial metabolism data.

ABSTRACT:

The usefulness of *Drosophila* as a model organism for the study of human diseases, behaviors and basic biology is unquestionable. Although practical, *Drosophila* research lacks popularity in developing countries, possibly due to the misinformed idea that establishing a lab and performing relevant experiments with such tiny insects is difficult and requires expensive, specialized apparatuses. Here, we describe how to build an affordable flylab to quantitatively analyze a myriad of behavioral parameters in *D. melanogaster*, by 3D-printing many of the necessary pieces of equipment. We provide protocols to build in-house vial racks, courtship arenas, apparatuses for locomotor assays, etc., to be used for general fly maintenance and to perform behavioral experiments using adult flies and larvae. We also provide protocols on how to use more sophisticated systems, such as a high resolution oxygraph, to measure mitochondrial oxygen consumption in larval samples, and show its association with behavioral changes in the larvae upon the xenotopic expression of the mitochondrial alternative oxidase (AOX). AOX increases larval activity and mitochondrial leak respiration, and accelerates development at low temperatures, which is consistent with a thermogenic role for the enzyme. We hope these protocols will inspire researchers, especially from developing countries, to use *Drosophila* to

easily combine behavior and mitochondrial metabolism data, which may lead to information on genes and/or environmental conditions that may also regulate human physiology and disease states.

INTRODUCTION:

Drosophila melanogaster was introduced to the scientific community as a potentially powerful model organism more than 100 years ago. That potential has been firmly validated in several areas of the biological and biomedical sciences, such as genetics, evolution, developmental biology, neurobiology, and molecular and cell biology. As a result, six Nobel Prizes in Medicine or Physiology have been awarded to ten *Drosophila* researchers who have substantially contributed to our understanding of heredity, mutagenesis, innate immunity, circadian rhythms, olfaction and development¹. Perhaps more importantly, *D. melanogaster* has not ceased to provide us with new models of human biology and diseases, as a quick search on PubMed reveals almost 600 publications in the last 5 years, using the search term “*drosophila* model” (², as of February, 2021). In the US, where *Drosophila* is a wide spread model organism in the biomedical community, about 2.2% of all R01 research awards granted by the NIH in 2015 were allocated to *Drosophila* researchers³. In Brazil, on the other hand, a search for currently funded projects on the website of the Sao Paulo Research Foundation (FAPESP), the most important funding agency for research in all scientific areas in the state of Sao Paulo, showed only 24 grants and fellowships with *Drosophila* as the main subject of study⁴. Considering all 13205 projects currently funded by FAPESP (⁵, as of February, 2021), those 24 *Drosophila* projects represent a ratio of less than 0.2% of the total projects, which is nearly 12 fold lower than that of the NIH. If we remove the funded projects that aim at studying *Drosophila* from an ecological and/or evolutionary point of view, and assume that the remaining projects use this organism as a model for understanding human biological processes in health and disease, that ratio decreases to a shocking ~0.1%.

In fact, a proper investigation is warranted to reveal the reasons why *Drosophila* research in Brazil/Sao Paulo does not appear to be as significant in number of funded projects. Culturing *Drosophila* is not expensive⁶⁻⁸ and is relatively simple, as unlike vertebrates, no permission from a bioethical committee is necessary for experimentation^{9,10}. An approval to work with genetically modified fly lines is, however, required in Brazil¹¹, adding a layer of bureaucracy inherent to all work involving genetically modified organisms. However, this would likely not prevent interested researchers from initiating a flylab. We speculate that misinformation about the power of the model, and about the expected high costs associated with setting up a flylab and performing meaningful experiments are important factors in this decision. As for most science equipment and supplies, the appropriate apparatuses to perform general fly maintenance and behavioral analyses must be imported into Brazil from North America, Europe and/or elsewhere, which is an expensive and extremely time consuming process^{12, 13}.

Recently, an alternative to importing specialized apparatuses has emerged as 3D printers have become more affordable and accessible to any person, including *Drosophila* researchers in developing countries. The 3D-printing technology has been widely used in the last 10 years by members of the "maker culture", which is based on the idea of self-sufficiency over exclusively relying on company manufactured products¹⁴. Such an idea has always been present in academic

research laboratories around the globe, so it is not surprising that 3D printers have become standard lab equipment in many places^{15, 16}. For a number of years, we have been 3D-printing fly vial racks, mating arenas, climbing apparatus, among other devices, for a fraction of the cost of brand-named equivalents. The reduced costs of printing and assembling homemade lab equipment is classically represented by the FlyPi, which can be built for less than €100.00 and serves as a light and fluorescence microscopy able to use sophisticated opto- and thermogenetic stimulation of the genetically tractable zebrafish, *Drosophila* and nematodes¹⁵. Here, we provide a series of protocols for anyone interested in becoming a *Drosophila* researcher (or in expanding his/her own existing flylab) to 3D-print many of the necessary material. By investing time and developing a little expertise, the reader will even be able to optimize the protocols presented here to print apparatuses better adapted to his/her own research needs.

However, a flylab is not a place for “cheap” equipment only, especially when one intends to associate behavioral analyses with underlying metabolic phenomena. We have also been interested in the roles of mitochondria in the modulation of *Drosophila* behavioral patterns, as these organelles are responsible for the bulk production of ATP in most tissues through several metabolic pathways whose products converge to oxidative phosphorylation (OXPHOS). Analyzing mitochondrial oxygen consumption as a way to understand mitochondrial metabolism does require an oxygraph, which is a more sophisticated piece of equipment that unfortunately cannot yet be 3D-printed. Because OXPHOS impacts practically all cellular processes since it depends on a series of exergonic redox reactions that occur in the cell^{17, 18}, oxygen consumption rates based on the oxidizable substrate provided to mitochondria may help reveal whether the organelle’s functioning is cause or consequence of a particular behavior. Therefore, we also provide here a protocol for measuring mitochondrial oxygen consumption in larva samples, as we realize the vast majority of published protocols are focused on analyzing adult samples. We show that changes in mitochondrial respiration, induced by the transgenic expression of the *Ciona intestinalis* alternative oxidase (AOX), leads to increased larval mobility under cold stress. This is most likely due to thermogenesis, since AOX is a non-proton pumping terminal oxidase that can bypass the activity of OXPHOS complexes III and IV (CIII and CIV), without contributing to the mitochondrial membrane potential ($\Delta\Psi_m$) and ATP production^{19–21}. No insect, including *Drosophila*, or vertebrate naturally possesses AOX^{21–23}, but its expression in a myriad of model systems^{24–29} has been successful to show its therapeutic potential for conditions of general mitochondrial respiratory stress, especially when caused by CIII and/or CIV overload. AOX confers resistance to toxic levels of antimycin A²⁴ and cyanide^{24, 25}, and mitigates diverse phenotypes related to mitochondrial dysfunction^{24, 25, 30–32}. The fact that AOX expression changes larval behavior and mitochondrial function justifies more in-depth studies of this enzyme’s roles in the metabolism and physiology of metazoan cells and tissues^{33, 34}.

We hope that with this article we can help raise awareness within the scientific community of developing countries such as Brazil that using the excellent genetic toolset that *D. melanogaster* presents, in combination with efficient and affordable homemade apparatuses for behavioral analyses, can generate relatively fast basic research data on interesting biological processes with significant translational impact, supporting future therapeutic studies in clinical research. Developing such communal ideals would greatly benefit Drosophilists, medical researchers, and

the biological and biomedical sciences. Most importantly, it would benefit society in general, as public funding could be applied more translationally to understand and treat human diseases. The protocols we provide here for 3D printing the apparatuses for a flylab were designed for use with the RepRap 3D printer, based on the Prusa I3 DIY model available at ³⁵. We use the 1.75-mm white polylactic acid (PLA) filament (SUNLU) as raw material for printing, the Tinkercad platform³⁶ for model design, and the Repetier-Host software³⁷ for STL to G-Code conversion, a necessary step to provide coordinates to the printer. Further optimization of the protocols is required should the reader want to use alternative equipment, materials and software.

PROTOCOLS:

1. 3D model design

NOTE: The workflow for 3D printing has three basic steps: (1) 3D modeling; (2) importing the model into the slicing software; and (3) selecting the correct filament, configuring the printer, and finally, printing. A basic protocol for modeling a small fly vial rack/tray is shown below; this rack is to be used with standard fly vials, which have approximately 2.5 cm in diameter and 9.8 cm in height. For new model designs, the tools provided by the Tinkercad software allow the easy handling of three-dimensional structures, by creating pieces of different shapes, sizes and thickness, according to one's own needs. For Drosophilists venturing for the first time into the realm of 3D printing, following the protocols below, even with all their details, may still be challenging, so we strongly recommend becoming acquainted with the software for best results.

1.1. Sign in to Tinkercad online³⁸ (**Figure 1A**). Prior registration with personal information is required to access the platform, free of charge.

1.2. Click on **Create a new Project** to begin a new design, and rename the Project accordingly on the upper right corner of the window. Press **Enter** to be directed to the project's workplane (**Figure 1B**).

1.3. Verify if the workplane has the correct dimensions of 200 mm x 200 mm, by clicking with the mouse's left button on **Edit Grid** at the lower right corner (red square in **Figure 1B**). In the popup window (**Figure 1C**), make sure that the "Units" are millimeters, and the "Presets" are default. Enter 200.00 in the "Width" and in the "Length" fields, and click on **Update Grid** to save the changes.

1.4. Verify if the **Snap Grid** is set to 1.0 mm (red square in **Figure 1B**). If it is not, click on the dropdown menu and select 1.0 mm.

1.5. Under the Basic Shapes menu on the right (blue square 2 in **Figure 1B**), select a solid box and drag it to the center of the workplane.

1.6. Click anywhere on the box in the workplane with the mouse's left button to see its edges and vertices. Click on any vertex (which will then turn red) to show the box dimensions

(red squares in **Figure 1D**). Click with the mouse's left button on each dimension and type 130 mm for length (L), 130 mm for width (W) and 40 mm for height (H). Recenter the box by dragging it to the middle of the workplane.

1.7. Click on the tool **Ruler** on the upper right corner of the screen (red square 1 in **Figure 1E**). Immediately click on the lower left vertex of the box, as indicate in **Figure 1E** (red square 2), to set the initial point ($x = 0$, $y = 0$, $z = 0$) of a tridimensional Cartesian coordinate system. Note that the distance between the selected vertex and the coordinate initial point will now show (red squares in **Figure 1F**), where "A" "B" and "C" represent the distance to the x, y and z axes (which should be zero in this case), respectively.

1.8. Next, select an empty (hole) box from the **Basic Shapes** menu on the right (blue square 2 in **Figure 1B**) and drag it to the workplane. Set its dimensions to 30 (L) x 30 (W) x 40 (H) mm, and elevate it 2 mm from the workplane, by typing "2.00" in the textbox next to the green arrowhead on the lower right corner of the empty box (red square in **Figure 1G**). Position the empty box inside the solid box 2 mm away from the x,y coordinate initial point, by typing "2.00" in the textboxes next to the green arrows on the lower left corner of the box (red squares in **Figure 1H**; compare with **Figure 1G**).

1.9. With the empty box still selected, press the **Ctrl+D** keys on the keyboard to deploy the "duplicate" command and create a new empty box of the exact same dimensions. Position the new empty box inside the solid box, next to the first empty box, by typing "34.00" in the textbox next to the green arrow along the y axis, and "2.00" in the textboxes next to the two remaining green arrows (red squares in **Figure 1I**).

1.10. Repeat this step, adjusting for the correct distances from the coordinate initial point, until the entire solid box is filled with empty boxes spaced 2 mm apart from each other (**Figure 1J**).

1.11. Select all the boxes (solid and empty ones) by clicking with the mouse's left button and dragging to the entire area. Press the **Ctrl+G** keys on the keyboard to deploy the "group" command and create a single box with 16 empty spaces for fly vials (**Figure 1K**). This is the final design of the vial rack.

1.12. Click on **Export** on the upper right corner of the Tinkercad window. On the window box displayed (**Figure 1L**), select **Everything in the design** next to **Include**, and **.STL** under **For 3D Print** as the file type. Choose a proper name for the design file and save it in an appropriate place in the computer.

2. 3D printing

NOTE: In this section, we provide instructions on how to use the STL file created in Step 1 and convert it to the G-Code file containing the printing instructions to the 3D printer. This is the slicing process, for which we use the Repetier-Host software.

2.1. Download **Supplemental File 1** and save it on an appropriate place in the computer. This is a .rcp file containing the printer configurations to be used below. To get more information on the .rcp file type, please visit ³⁹.

2.2. Open the Repetier-Host software, which should already be installed on the computer, following instructions from³⁷. Press the **Ctrl+O** keys on the keyboard to open the STL file on the computer created in step 1.

2.3. Once opened, click on the designed vial rack and press the **R** key on the keyboard to open the editing menu on the right side of the screen (red square 1 in **Figure 2A**). Centralize the object on the printing table by clicking on the **Center Object** button, indicated with red square 2 in **Figure 2A**, on the **Object Placement** tab.

2.4. Click on the **Slicer** tab (red square 1 in **Figure 2B**) next to **Object Placement** tab, and then click on the **Configuration** button (red square 2 in **Figure 2B**) below. Note that a new window on the left will open where the printer parameters such as velocity, layer thickness and holders can be defined (see more details in the Discussion below).

2.5. Click on the **Import** button (red square 3 in **Figure 2E**), select **Supplemental File 1** from the files, and press **Enter**. Note that this .rcp file (downloaded in step 2.1) provides the parameters for the automatic configuration of the printer we have optimized for this vial rack.

2.6. To finish configuring the printing parameters, select **None** for Support Type on the menu on the right (red square 4 in **Figure 2E**), as printing of this piece does not require a support to prevent bending or other deformities. In **Infill Density** (red square 5 in **Figure 2E**), choose 20% to create a solid structure (see more details about these parameters in the Discussion below).

2.7. Click on **Slice with CuraEngine** on the upper right corner of the screen to run the slicing program and generate the G-Code, which has the information necessary for the printer to print the piece. Note that under the **Print Preview** tab on the menu on the right (next to the **Slicer** tab), information about the time and amount of material required for the printing job to be completed will then show (red square 1 in **Figure 2F**).

2.9. Click on **Save for SD Print** to save the G-Code file in a SD card (red square 2 in **Figure 2F**). Note that the G-Code contains the 3D coordinates of the designed piece, sliced into layers, for proper function of the printer.

2.10. Insert the SD card in the RepRap 3D printer, and then follow the information displayed on the printer screen to select printing from the SD card.

2.11. Select the G-Code file of the vial rack. Note that the printer will automatically warm up and start printing the designed piece, which should take several hours. The rack (**Figure 3A**) should be ready for use immediately after the printing job is completed.

3. Behavioral analysis apparatuses

NOTE: The steps described in steps 1 and 2 can be repeated with appropriate adjustments to print several of the pieces of lab equipment needed. However, we realize that designing new pieces may be challenging and time-consuming for beginner users of Tinkercad, so instead of providing step-by-step protocols on how to design all models, we are making available for download several design models we created as STL files (see **Supplemental Files 2-11**).

3.1. Download **Supplemental File 2** for a model of a small funnel (**Figure 3B**), routinely used in flylabs to help transfer adult flies to new vials or bottles by avoiding flies crawling up the inside walls of these containers to escape.

3.2. Download **Supplemental File 3** for a tapping mat support (**Figure 3C**), which can hold an ethylene-vinyl acetate foam or a thick cotton mat which glass vials or bottles can be tapped onto when one is tipping flies into new containers with freshly made food.

3.3. Download **Supplemental File 4** and **Supplemental File 5** for the model of a camera stand that we named Stalker (**Figure 3D**).

NOTE: The apparatus allows any camera (professional, webcams, cellphones, etc.) to be positioned on top of a base where a Petri dish containing larvae or adult flies can be imaged or video recorded. Stalker allows the imaging of animal behavior that takes place horizontally, always at the same distance from the Petri dish, which avoids introducing variability into the experimental measurements if the recordings must be made on different days, for example, or if the camera needs to be used for another purpose in between recordings. The apparatus is conveniently modular and can be easily assembled after printing the base and the top from **Supplemental File 4**, and the sides from **Supplemental File 5**. The 1 cm² squares at the base, which can be highlighted using a permanent marker, help track distance travelled by individual animals. Print the apparatus (at least the base) using white filament, so that there is enough contrast between the background and the animals for the tracking software to identify each fly.

3.4. Download **Supplemental File 6** for the printable design of the Fly Motel (**Figure 3E**), which has ten courtship and mating arenas (rooms) organized in a manner to facilitate video recordings of ten individual mating pairs at a time. Note that the Fly Motel is based on the device published in ⁴⁰, where detailed explanation for its use in behavioral studies is found. In addition to the 3D-printed parts, the apparatus requires 12 screws (3 x 8 mm) for fixing the upper part to the lower one to stabilize the assembled device, an acrylic plate (60 x 60 x 3 mm), and a zip tight. Because the structure of the Fly Motel is more complex, we also provide an instructional video (**Supplemental File 7**) of how to assemble it correctly, given that all required pieces and a screwdriver are available.

3.5. Download **Supplemental File 8** for the model of a T-Maze (**Figure 3F**), which is used for memory assays using adult flies. A detailed explanation of how the T-Maze is used to make flies

associate repulsive odor stimuli with their phototropic behavior is found in the original publication⁴¹. The apparatus also makes use of two translucent 15 mL conical tubes, which are commonly found in any lab and are attached to the 2 cm-wide circular openings in each side of the central piece. Note that the printing of the T-Maze requires a support (see more details in the legend to **Figure 2**). Select “Everywhere” for Support Type (red square 4 in **Figure 2E**) after following steps 2.1-2.6 above.

3.6. Download **Supplemental File 9** and **Supplemental File 10** for the design of the printable parts of our version of the apparatus for rapid iterative negative geotaxis (RING) assays (**Figure 3G**), used to perform climbing assays with adult flies of several genotypes or environmental conditions simultaneously, generating results in a more standardized and higher-throughput fashion⁴². The RING apparatus is also modular, and in addition to the 3D-printed parts, it requires other pieces that can be easily purchased online or in a hardware store at low cost: two $\Phi 8 \times 300$ mm rectified shafts, four $\Phi 8$ mm linear bearings, rubber bands (or pieces of a string), a 240 x 60 x 20 mm piece of wood for the base, and eight wood screws (8 mm) to fix the printed parts to the wood base. Download **Supplemental File 11** for instructions on how to assemble the device once all parts are printed or purchased. A detailed explanation of how to use the RING apparatus is found in the original publication⁴².

4. Larval mobility assay

NOTE: We have optimized this protocol, originally based on Nichols et al.⁴², to study the effects of AOX expression on *Drosophila* development under cold stress. The lines *3xtubAOX*²⁵ and *w*¹¹¹⁸, used as examples of AOX-expressing and control larvae, respectively, were cultured on standard diet²⁴ at 12 °C, according to Saari et al.³⁴. We recommend this protocol to analyze the mobility of larval samples of any genetic condition, cultured under any environmental condition of interest.

4.1. Prepare 2% agar plates by boiling the equivalent amount of agar in deionized water, pouring into $\Phi 90 \times 15$ mm Petri dishes, and allowing them to solidify at room temperature. For plates with a final volume of 20 mL each, use 0.4 g of agar.

4.2. Carefully collect wandering L3 larvae from the side of the culture vials/flasks using a pair of round tip forceps or a brush, and place the individuals in a $\Phi 90 \times 15$ mm Petri dish with deionized water for less than 10 seconds to rinse food particles attached to their body.

4.3. Transfer individual larva to dishes with agarose and wait 5 minutes for the animals to acclimate.

4.4. Position the dishes containing the individual larva on top of a graph paper (0.2 cm² grid), and count the number of lines crossed by the animal for 1 minute, as it moves on top of the agar. Each line crossed represent a distance of 2 mm. Repeat the procedure with the same individual 10-15 times to obtain technical replicates.

4.5. Repeat step 4.4 with at least 8-10 individuals from different tubes/flasks, cultured at

different times to obtain biological replicates of the same line.

4.6. Repeat steps 4.4 and 4.5 to obtain data for the other fly line (or for as many lines as one intends to analyze).

4.7. The same individual larvae used in steps 4.4-4.6 may be used to obtain additional data on body movement by placing the agar dishes with an individual larva under a stereomicroscope and counting the number of peristaltic contractions of the body wall for 1 minute. Obtain technical and biological replicates for an estimate of average mobility among the fly lines analyzed.

4.8. Apply the statistical test to calculate the probability of the values of these larval mobility parameters being distinct among the lines of interest. Because we are comparing here data from only two lines, a Student's t test may be applied.

5. Mitochondrial respirometry using larval homogenates

NOTE: The following protocol was optimized to measure mitochondrial oxygen consumption from larval homogenates of the AOX-expressing line *3xtubAOX* and the control *w¹¹¹⁸*, cultured at 12°C, but we also recommend it to be used for larval samples of any genetic and environmental conditions. We realize that conducting such experiments should not be included as an “affordable” goal for a “home-made” flylab, unlike all other protocols we provide in this article, as a considerable initial investment must be made for a lab to acquire a high resolution oxygraph. The protocol is to be used with the Oxygraph-2k (O2k) and the DatLab software from Oroboros Instruments, so further optimization is required should the reader want to use an alternative equipment.

5.1. Turn on the O2k and start the DatLab software in the computer connected to the oxygraph. The magnetic bars inside the assay chambers should start stirring automatically. Remove the ethanol storage solution from the chambers.

5.2. Wash the chambers at least 3 times with 100% ethanol and 3 times with ultrapure water.

5.3. In DatLab, the window **O2k Control** will open automatically. In **Block temperature [°C]**, enter 12 °C (or the preferred temperature in the range of 2-47 °C) and press **OK**.

5.4. A second window, **Edit Experiment**, will then open automatically. Enter sample names in the **Sample** fields, according to what will be added in chambers A and B, and press **Save**.

5.5. Add 1800 µL of the assay buffer (120 mM KCl, 5 mM KH₂PO₄, 3 mM Hepes, 1 mM EGTA, 1 mM MgCl₂, 2% BSA, pH 7.4) in each chamber and close them partially, still allowing oxygen exchange with the outside air. Allow the oxygen concentration and oxygen flux signals to stabilize, showing minimal fluctuations for at least 10 min. This step will provide the calibration of the equipment with the outside air on the day of the experiment (see steps 6.3 and 6.4 below)

for further details on experimental calibrations).

5.6. During the air calibration step, initiate sample preparations by carefully collecting from the culture tubes/flasks 20 wandering larvae of the appropriate genotype, using a pair of forceps or a small paintbrush.

5.7. Rinse each larva quickly but thoroughly with deionized water or 1x PBS (137 mM NaCl, 2.7 mM KCl, 8 mM Na₂HPO₄ and 2 mM KH₂PO₄) and transfer them to a 1 mL glass homogenizer on ice, containing 500 µL of ice-cold isolation buffer (250 mM sucrose, 5 mM Tris HCl, 2 mM EGTA, pH 7.4)

5.8. Homogenize the whole larvae with 5 strokes and pour the homogenate into a 1.5 mL microcentrifuge tube on ice.

5.9. Add 300 µL of isolation buffer to the glass homogenizer, macerate the remaining larval tissues further with 3 strokes, and pour the homogenate again into the same microcentrifuge tube on ice.

5.10. Add 200 µL of isolation buffer to the glass homogenizer, macerate the residual larval tissues further with 2 strokes, and pour the homogenate again into the same microcentrifuge tube on ice.

5.11. Mix the final homogenate (~1 mL) by inverting the tube twice gently and keep it on ice until the second sample is processed.

5.12. Repeat steps 5.6-5.11 to obtain the larval homogenate of the other genotype.

5.13. Open the oxygraph chambers A and B, and transfer 200 µL of each homogenate to the assay buffer in each chamber, which must be exactly at 12 °C at this point. Close the chambers completely and allow the oxygen concentration and oxygen flux signals to stabilize for approximately 10 min.

5.14. Initiate oxygen consumption measurements by adding to each chamber 5 µL of a solution of 2 M pyruvate, 2 M proline (final concentration in the chambers = 5 mM each) and 7.5 µL of a solution of 0.4 M malate (1.5 mM). Allow at least 5 minutes for signal stabilization. Note that at this point, the mitochondria will be charged with oxidizable substrates to initiate the tricarboxylic acid (TCA) cycle reactions. Any increase in the oxygen consumption signal may be due to the functions of uncoupling proteins (or due to other uncoupling phenomena), and can be used to calculate general uncoupled respiration (also referred to as Leak respiration in the absence of adenylates, L_N – see Representative Results for details).

5.15. Add to each chamber 4 µL of a solution of 0.5 M ADP (1 mM) and allow at least 5 minutes for signal stabilization. A significant increase in the oxygen consumption signal is usually immediately observed, representing the oxidative phosphorylative (OXPHOS) respiration. The

great majority of this OXPHOS respiration is driven by complex I (CI).

5.16. Add to each chamber 2 μ L of a solution of 0.05 M antimycin A (0.05 mM) to inhibit CIII, and allow at least 5 minutes for signal stabilization. A decrease in the oxygen consumption signal down to the basal levels seen before the addition of pyruvate, proline and malate should be observed for the w^{1118} control sample. Mitochondrial respiration from AOX-expressing larvae will be partially resistant to antimycin-A, as the electrons can now be directed to AOX. About 40% of the total OXPHOS respiration should remain after CIII inhibition, which should be all supported solely by AOX.

5.17. Add to each chamber 4 μ L of a solution of 0.1 M propyl-gallate (0.2 mM) to inhibit AOX, and allow at least 15 minutes for signal stabilization. The oxygen consumption levels in the AOX-expressing larval samples should now decrease to the basal levels seen before the addition of pyruvate, proline and malate. This decrease proves that the antimycin-A resistant respiration observed is due to AOX function.

5.18. Add to each chamber 1 μ L 0.01 M rotenone (0.005 mM) to inhibit CI, and allow at least 5 minutes for signal stabilization to obtain the oxygen consumption signal of the sample independent of mitochondrial respiration. This signal is usually as low as that observed before the addition of pyruvate, proline and malate.

5.19. Save the experiment and close the DatLab software.

6. Mitochondrial respirometry data processing

NOTE: Oxygen consumption values are obtained as an average of the oxygen flux signals in a determined period of time and are expressed as pmol O₂ consumed per second per mg total protein in the sample. The values are first referenced against the maximal oxygen concentration available in the assay buffer on the day of the experiment, based on the experimental temperature (referred to as air saturation), and the minimal oxygen concentration, which is determined previously in each chamber by the addition of Na₂S₂O₄ to the assay buffer (see ⁴³ for the manufacturer's guidelines to obtain zero oxygen calibration). The values are also normalized by the amount of total protein in the larval homogenates added to the assay buffer of each chamber.

6.1. Determine total protein concentration of each sample using the Bradford method⁴⁴. Reopen the saved experiment on the DatLab software, press **Experiment** at the top menu, and then **Edit**. In the opened window, select **mg** in the **Unit** section and in the **Amount** section enter the protein amount contained in the 200 μ L of the sample added in each chamber. The concentration will be automatically calculated by the software, considering the total chamber volume of 2 mL. Press the **Save** button.

6.2. Press **Graph** in the top menu, and then **Select plots**. In the opened window, select **Flux per mass** for both graphs (1 and 2, which refer to chambers A and B, respectively). Press **Ok**. The

experimental outcome is now normalized by the protein concentration of the samples (pmol O₂/s/mg total protein).

6.3. On the upper right corner of each graph (1 and 2) of the main experimental outcome page, click on **O₂ Concentration**. Along the x axis, identify a time range prior to addition of the samples in the chambers, in which the oxygen concentration and flux signals are very stable.

6.3.1. Press and hold the Shift key on the computer's keyboard, click with the left mouse button on the initial time selected, drag the cursor along the time axis to select the desired region, and release the mouse button. Do this procedure for each of the graphs individually.

6.3.2. Double-click on the blue bars of the selected areas at the bottom of the graphs, and type "air" to indicate that these are the selected regions used to calculate the oxygen air saturation.

6.4. Click on **Calibration** on the top menu bar, and select **A: Oxygen, O₂** to calibrate chamber A. In the opened window, verify that **O₂ Calib** is selected (yellow color).

6.4.1. For the **Zero calibration**, click on **Copy from file** and choose the file with the previously performed zero oxygen calibration (see <https://www.oro-boros.at> for the manufacturer's guidelines).

6.4.2. For **Air calibration**, select **air** in the **Select Mark** column. Click on **Calibrate and copy to clipboard**.

6.5. Click on **Calibration** on the top menu bar, select **B: Oxygen, O₂** and repeat step 6.4 to calibrate chamber B.

6.6. On the upper right corner of each graph (1 and 2) of the main experimental outcome page, click on **O₂ flux per mass**. Select desired stable regions of the oxygen consumption signal by holding the Shift key on the keyboard, clicking with the left mouse button, and dragging the cursor along the time axis. The stable regions selected between additions of pyruvate/proline/malate and ADP represents the L_N ; between ADP and antimycin A, OXPHOS; between antimycin A and propyl gallate (upon CIII inhibition), antimycin A-resistant respiration; between propyl gallate and rotenone (upon CIII+AOX inhibition), residual respiration; after rotenone (upon CI+CIII+AOX inhibition), residual non-mitochondrial respiration. Double-click on the red bars of the selected areas at the bottom of the graphs, and enter appropriate labels.

6.7. Click on **Marks** on the top menu bar, and then **Statistics**. In the **Show** tab of the opened window, uncheck all options except **O₂ flux per mass**. In the **Select** tab of the same window, select chamber A to obtain the respiration data for the first sample. Click on **Copy to clipboard** and paste the data into a spreadsheet. Repeat the procedure to obtain the data for the second sample in chamber B.

6.8. In a spreadsheet, subtract all respiration values by the residual non-mitochondrial respiration

(the data after rotenone addition). Calculate averages from multiple experimental replicates and plot the data as preferred.

REPRESENTATIVE RESULTS:

By following the steps in steps 1 and 2, one should be able to design a simple fly vial rack, and run the model STL file through the slicing program to generate coordinates for the 3D printer. **Figure 3A** shows a printed unit of the model next to its design. We also hope step 1 can provide the basic skills for one to use the basic shapes available in the Tinkercad platform to create useful apparatuses for the lab. Developing these skills, however, may require constant practice and frequent consultations of the Tinkercad help center⁴⁵. In step 3, we provide our own designs for apparatuses that we routinely use for general fly maintenance and behavioral studies with adults or larvae. By following step 2, a researcher should be able to use the STL files provided as **Supplemental Files 2-6** and **8-10** in step 3 to print tapping mat supports, funnels, Stalkers, Fly Motels, T-Mazes and RING apparatuses. **Figure 3B-G** shows side-by-side images of the model designs and of the actual printed and assembled apparatuses. It is important to mention that each printer may require minimal adjustments to the printing settings for optimal function; our **Supplemental File 1**, however, appears to provide a robust initial set of instructions for RepRap 3D printers to print the abovementioned devices.

In addition to providing instructions on how to create and 3D-print apparatuses that can be used for behavioral analyses in *Drosophila*, we also provide a protocol to perform assays and obtain behavioral measurements using larvae (step 4) and a protocol for high resolution respirometry using larval homogenates (steps 5 and 6) to investigate mitochondrial metabolism. The mobility assays provided can easily reveal the impact on larval behavior at cold temperatures, when the fly OXPHOS is directly altered by ubiquitous expression of AOX. AOX-expressing larvae can cover distances ~70% longer than control larvae at the stressful temperature of 12 °C (**Figure 4A**), apparently due to the ~40% higher number of peristaltic movements of the body wall (**Figure 4B**). We can also easily associate this change in behavior with changes in mitochondrial function. **Figure 5A** shows the traces of oxygen consumption as a representative outcome of an experiment using larval homogenates. It is evident that the mitochondria of AOX-expressing larvae have antimycin A-resistant respiration, which is sensitive to the AOX inhibitor propyl-gallate (green arrow in **Figure 5A**, and **Figure 5B**), and consistent with previously published data using adult flies and the expected function of AOX²⁴. Quantification of the different oxygen consumption states also indicates that L_N respiration is elevated in AOX-expressing larvae (**Figure 5B**). This in turn is reflected in the calculations for respiratory control ratio (RCR), which is a parameter that indicates how coupled mitochondria are by dividing the values for OXPHOS respiration by those of Leak respiration^{46, 47}. The lower RCR in AOX-expressing larvae suggests mitochondria are less coupled in these flies (**Figure 5C**). We speculate that the energy that is not being used for ATP synthesis is in fact being dissipated as heat, which gives AOX-expressing larvae more mobility at such an extremely stressful temperature.

FIGURE AND TABLE LEGENDS:

Figure 1. Modeling of a small fly vial rack using Tinkercad. (A) Access to the modeling platform is given online³⁸ using the user's preferred password-protected credentials. (B) General view of

the platform. Blue square 1 indicates the workplane, which represents the printer table, where objects are designed. Blue square 2, Basic Shapes menu, where several pre-made shapes are found. Blue square 3, a menu with useful functions, such as mirror, copy, duplicate and combine. Blue square 4, workplane movement menu, which controls rotations of the workplane to better view the object being modeled. Positioning the side of the cube using the mouse's left button to "Top", "Bottom", "Front", "Back", "Right" and "Left" shows views of the object from different angles. Blue square 5, left menu containing other useful functions, such as zoom in and zoom out, among others. Red square, "Edit Grid" and "Snap Grip" options. (C) The Edit Grid window, where the workplane can be edited. (D) The design of a solid box (future vial rack). Red squares indicate the textboxes in which the dimensions of the box can be typed. (E) The design of a solid box (future vial rack) of 130 (length) x 130 (width) x 40 (height) mm. Red square 1 indicates the tool "Ruler"; red square 2, the lower left vertex of the box, which will become the initial point ($x = 0$, $y = 0$, $z = 0$) of a tridimensional Cartesian coordinate system. (F) The same solid box as in E, with red squares A-C illustrating that the lower left vertex of the box is now 0.00 mm away in all axes from the initial point of a tridimensional Cartesian coordinate system. (G) An empty (hole) box (future space for a fly vial) of 30 x 30 x 40 mm is inserted in the workplane. The red square indicates the textbox in which 2.00 should be typed to elevate the empty box 2 mm from the workplane. (H) The same empty box as in G is positioned inside the initial solid box of 130 x 130 x 40 mm by typing 2.00 in the textboxes indicated with red squares. (I) A second empty box inserted into the design illustrates how the spaces for fly vials are created one by one, based on the first empty box. The red squares indicate the textboxes that must be filled for the proper positioning of the empty boxes. (J) The design is now filled with 16 empty boxes, evenly spaced inside the initial solid box. (K) Final 3D model of the vial rack, which is now a single piece, created by grouping the initial solid box with the 16 empty boxes evenly spaced inside the solid box. See Step 1 for details on the whole procedure, including how to save the final model as an STL file (L).

Figure 2. Slicing of the 3D vial rack model and configuring the printer using Repetier-Host. (A) The STL file containing the model of the vial rack (see Step 1 and **Figure 1** for details) is opened with the Repetier-Host software installed on the computer. The editing menu on the right is indicated by red square 1, and the Center Object button by red square 2. (B) Initial steps to run the slicing software (see Step 2 for details). Red square 1 indicates the Slicer tab on the editing menu; red square 2, the Configuration button; red square 3, the Speed and Quality window, where important printer parameters such as velocity, layer thickness and holders can be defined (see the Discussion for details). (C) Detail of the Speed and Quality window. The red square indicates where the thickness of the printing layers (Layer Height and First Layer Height) can be adjusted. (D) In the Filament tab (red square), one is able to check parameters related to the filament to be used, such as the Diameter (which for most filaments is set to 1.75 mm), the Print and Bed Temperatures (respectively, the temperature to melt the filament at the printer extruder, and the temperature of the printer table which helps with adherence), and the Cooling Speed (which in general guarantees that the extruder does not overheat). (E) Final steps to run the slicing software (see step 2 for details). Red squares 1 and 2 same as in (B); red square 3, the Import button, where most of printer's adjusting parameters can be uploaded from **Supplemental File 1**; red square 4, Support Type option, which in this particular case of the fly rack should be "None"; and red square 5, Infill Density option, which should be 20% for printing

of most objects. The use of a support, such as for the printing of the T-Maze (see step 3 for details), is necessary when the layers are not to be printed directly onto the printer table or on top of another layer. The support is particularly important to prevent collapse of structural parts that are in an arc format or of closed structures that are hollow inside, for example. (F) Visualization of the printing statistics (red square 1) under the Print Preview tab, which is calculated after the **Slice with CuraEngine** button (shown in E) is pressed. After pressing the **Save for SD Print** button (red square 2), the G-Code file should be saved in an SD card to be transported to the printer.

Figure 3. “Homemade” apparatuses for general fly maintenance and behavioral analyses. Side-by-side images of our model designs (left) and of the actual printed apparatuses (right) are shown: small fly rack (A), funnel (B), tapping mat support (C), Stalker (D), Fly Motel (E), T-Maze (F), and RING apparatus (G). Details on how to print and assemble these apparatuses are shown in steps 1-3. Note that in F, the picture of the T-Maze does not contain the two 15 mL conical tubes which would give it its “T” shape⁴¹.

Figure 4. Higher mobility of AOX-expressing larvae cultured at 12 °C. Measurements of distance crawled (A) and number of body wall contractions (B) per minute by individual larva were obtained as described in step 4. The fly lines used were w^{1118} (control, AOX-nonexpressor) and $3xtubAOX$ (AOX-expressor)²⁵. Datapoints indicate means \pm standard deviation of 8 biological replicates with 15 technical repetitions each. * indicates significant differences ($p < 0.01$), according to a Student's t-test.

Figure 5. Higher levels of mitochondrial oxygen consumption in AOX-expressing larvae cultured at 12°C. (A) Traces of a representative experiment showing changes in real time oxygen consumption (red line) and oxygen concentration (blue line) in the chambers as the indicated substrates and inhibitors were added (black arrows) to the assay medium containing whole larva homogenates of the w^{1118} (control, AOX-nonexpressor) and $3xtubAOX$ (AOX-expressor). Pyr+Pro+Mal indicates addition of pyruvate, proline and malate, which are oxidized inside mitochondria providing NADH, substrate for complex I. The following increase in oxygen consumption is due to Leak respiration without adenylates (L_N). Addition of ADP allows the ATP-synthase to release the proton gradient so that the Oxidative Phosphorylative respiratory state (OXPHOS) is achieved. Addition of antimycin A inhibits complex III (CIII), completely abolishing oxygen consumption in the AOX-nonexpressing control sample (top graph), and allowing the antimycin A-resistant respiration activity of AOX (green arrow) to be measured in the AOX-expressing sample (bottom graph). Addition of propyl-gallate, an AOX inhibitor, followed by the complex I inhibitor rotenone, certifies that mitochondrial respiration is totally abolished in both lines, allowing baseline oxygen consumption to be established. The first 50-60 min of the experiments, prior to the addition of Pyr+Pro+Mal, show the traces during stabilization of the oxygraph system, and were deliberately omitted here. The traces before addition of the sample homogenates are used for calculation of air oxygen saturation (see steps 5 and 6 for details). (B) Quantification of the oxygen consumption data shown in A averaged with that of 3-5 other biological replicates (\pm standard deviation). AA-resistant, antimycin A-resistant respiration; CIII + AOX inhibition, residual respiration. (C) Respiratory control ratio (RCR) was calculated as the

average ratio between OXPHOS and L_N respirations of the data shown in B and that of 3-5 other biological replicates (+/- standard deviation), to estimate mitochondrial OXPHOS-coupling efficiency. We have previously measured Leak respiration in the presence of oligomycin (L_{Omy}) and determined no differences between L_{Omy} and L_N (data not shown). Using L_N to compute RCR allows us to measure the antimycin A-resistant respiration by AOX in the same experiment. * indicates statistical differences ($p < 0.05$), according to Student's t-tests.

DISCUSSION:

The 3D-printing protocols and STL files provided here are intended to facilitate the setup of a new flylab or to increase the repertoire of apparatuses in an existing *Drosophila* behavioral facility, using “homemade” equipment. The 3D-printing strategy may be particularly useful in developing countries such as Brazil, where research using *Drosophila* as a model organism for studying human biology appears to be underrepresented, and specialized equipment is costly. Our protocols provide instructions on how to create the plastic framework and to assemble relatively simple devices, such as vial racks and apparatuses for memory, courtship and climbing assays, which may only need extra simple non-printable pieces for complete functionality. For proper printing results, the user may need to adjust a few printing parameters based on his/her own printer. In **Figure 2B**, under “Speed and Quality” (red square 3), one can find important settings that may determine the quality of the final printed piece. “Print” controls the range of speed at which the printer extruder works to form the 3D piece; the lower the speed, the higher the final quality and the total time needed to complete the job. In “First Layer”, one should consider the printing speed of the layer that will be placed directly onto the printer table. It is important that this is slow (30 mm/s), as any imperfections in the first layer may alter all of the layers above, causing deformities in the final piece. For the same reasons, we choose higher thickness for the first layer (“First Layer Height: 0.3 mm”), whereas the remaining layers can be thinner (“Layer Height”, red square in **Figure 2C**) without detracts to the final piece.

As the interested *Drosophilist* becomes more familiarized with the 3D-printing methods by creating the devices presented here, we recommend him/her to invest in more complex equipment that can provide more streamlined quantitative data for different behavioral parameters. One such equipment includes the FlyPi¹⁵, which is a relatively affordable, open-source platform for measuring behaviors of small model animals, including *Drosophila*, that can be controlled by optogenetic and/or thermogenetic tools, due to the attached LED-based fluorescence microscope and the Peltier-based temperature stimulator modules. Another example of a more sophisticated equipment that can be home-made is the ethoscope⁴⁸, a platform for high-throughput, real-time tracking and profiling of small animal behavior. For these, nevertheless, one must also invest in electronic components, such as cables, circuits, cameras, lens, among other parts, and follow the instructions provided by the original designers to assemble the parts into the 3D-printed framework and connect with the software^{49, 50}.

Among all model designs we present here, those for the tapping mat support and the funnel appear to be basically dispensable for a *Drosophilist* in a developed country. However, it is important to emphasize that basic supplies for a flylab in Brazil are not easily purchasable. For example, we are not aware of any company that produces polypropylene fly vials and bottles in

the country; these usually serve a single-use purpose in flylabs. They must then be imported and, as a result, they are relatively expensive and rarely ready for delivery when available in the national market. The large number of local companies that do glasswork, however, can easily provide us with customized reusable glass vials and bottles (such as those used by Thomas Hunt Morgan in the original Fly Room), which must be carefully cushioned when tapped to avoid breaking. Tapping mats and their supports are therefore extremely useful. We have not been able to 3D-print fly vials and bottles efficiently, as the printed pieces are not transparent enough for proper observation of the flies inside, even when using transparent filament (data not shown). Recently, the company Polymaker developed the Polysmooth, a filament designed specifically for post-processing and removal of the printing layer lines, allowing the printed devices to have a high degree of transparency. This may be extremely useful for printing fly vials in the future. Regarding funnels, although inexpensive and easily found in any supermarket or hardware store, they often have long tips and round cups, which are impractical for use in the lab. In this case, 3D-printing provided us with funnels customized for our needs.

Device customization is perhaps the most important aspect of the 3D-printing strategy, which can be employed by flylab members in developed and developing countries alike. We in fact have also customized the Fly Motel, the T-Maze and the RING apparatus, whose original designs were published elsewhere^{40–42}. The original Fly Motel design, for example, has more arenas and is therefore significantly larger in size⁴⁰. Printing such large apparatus would not have been feasible using our RepRap printer because of the limited space of its printing table (20 cm x 20 cm). In addition, recordings encompassing all individual arenas of the original Fly Motel design simultaneously would have generated poorer quality videos using our cameras, which could compromise software tracking of the individual animals and, ultimately, the behavioral analysis of the pair of flies in each individual arena. Moreover, the Fly Motel and the framework of the T-Maze were originally designed to be made of acrylic, which is significantly more expensive and allows less flexibility when assembling a modular apparatus; in other words, the actual acrylic pieces must have the exact size shown in the design, so that they can fit, assemble and form a single device⁴⁰. Instead, the PLA-printed pieces of the Fly Motel and the T-Maze are rigid, yet show some flexibility during assembly, in addition to having no known toxicity. 3D-printing the T-Maze using PLA also has another advantage over acrylic, as the former does not allow ambient light to penetrate the chamber inside the apparatus, allowing the flies to properly choose either of the two lateral conical tubes where the light should in fact play its essential role in these behavioral assays⁴¹.

Although simple, the Stalker is our own creation, designed to be very versatile. In addition to using it with any camera available as a stand-alone device so videos and pictures of flies can be made and analyzed on independent software, such as ImageJ⁵¹, it may also serve the purpose of a removable appendment to our own version of the ethoscope, by inserting it into the latter's internal recordable space. The STL files we make available with this article can be opened with Tinkercad to be even further altered with relative ease, before the interested researcher decides to 3D-print any of the devices, including our original Stalker. We make ourselves available by email to clarify any particular steps of our protocols, and to help with new designs of interest. We also encourage the reader to find important information on websites of “makers culture”

communities dedicated to design and produce lab equipment that is affordable for biologists in general: the Open Neuroscience⁵² and the 3D Printable Science⁵³.

We recognize that even with all the designed apparatuses presented here, some behavioral assays still need to be performed “manually”. Although this may introduce artifacts and subjectivity, it allowed us to analyze parameters that cannot be easily quantified using open-source software we have in our lab, such as the peristaltic movements of the larva body wall. Automated measurements of these movements can, however, be made using the FlyPi platform¹⁵. To test how the introduction of the non-proton pumping terminal oxidase AOX into the fly’s OXPHOS system may influence behavior, we made use of manually counting larval peristaltic movements under the microscope. Because we used the extreme temperature of 12 °C and larval mobility is usually very limited under these conditions^{54, 55}, manually measuring the distance travelled by the larvae along with counting body wall contractions turned out to be entirely feasible. We have shown previously that larval development is faster and larval viability is higher when AOX is expressed in flies cultured under stressful low temperatures, with more pronounced results at 12 °C³⁴. The hypothesis to explain these was based on the known thermogenic properties of plant AOX^{56–58}: the enzyme activity uncouples mitochondria, generating heat and consequently accelerating larval metabolism. Showing here that AOX-expressing larvae are significantly more mobile at 12 °C (**Figure 4**) is consistent with such a hypothesis.

Also consistent with the thermogenesis hypothesis is our mitochondrial respirometry data (**Figure 5**). We first developed the mitochondrial oxygen consumption protocol described here to be used with larval homogenates in an Oroboros O2k oxygraph at 12 °C. Condensation on the outside of the chambers due to the colder temperature inside was an initial concern for the long-term function of the equipment, but this does not appear to have caused any significant changes in the oxygraph performance throughout several years of use (data not shown). The use of total larval homogenates provides us with an estimate of mitochondrial performance in general, which is an important step when ubiquitously expressing AOX. Unlike respirometry experiments using whole adult homogenates, in which the flight muscle mitochondria are the most abundant mitochondria in the samples^{59, 60} the tissue(s) that most contribute(s) to mitochondrial respiration in larval homogenates has(ve) not yet been determined experimentally. Our protocol may certainly be advantageous in the pursuit of this goal, and in the investigation of the possible AOX-driven thermogenesis in a tissue-specific fashion. Using whole larva homogenates, however, requires significantly more cleaning and maintenance of the O2k chambers and oxygen sensors for proper continuing function of the equipment. We recognize that the high abundance of lipids and proteins stored in larvae is an important issue, as these with time may deposit on the interior walls of the assay chambers. Frequently, we have to clean the chambers with concentrated hydrochloric acid for completely removal of these deposits, following instructions from the manufacturer’s website⁴³. This process is time-consuming as the chambers must be removed from the equipment for a whole day of cleaning, and the equipment must be recalibrated when reassembled. This is, nevertheless, extremely important to prevent accumulation of lipid-soluble mitochondrial inhibitors that may interfere with the oxygen consumption assays.

Here, we measured three mitochondrial respiratory conditions in the presence of substrates whose oxidation provides electrons to CI, which in turn are finally used for O₂ reduction in the cytochrome c segment of the respiratory chain (CIII and CIV) or by AOX. L_N is sustained by electron transfer through these complexes and AOX, as a result of proton leakage from the mitochondrial intermembrane space to the matrix (intrinsic uncoupling). The OXPHOS condition is sustained basically by the same electron transfer reactions, which is in this case stimulated by the action of the ATP synthase, as it permits the dissipation of the proton gradient and the condensation of ADP and inorganic phosphate (coupled respiration)⁶¹. The antimycin A-resistant respiration, however, is similar to OXPHOS, but driven solely by AOX as the terminal oxidase. AOX-expressing larvae present strong antimycin A-resistant respiration (**Figure 5A and B**), which allows the development of these flies in food containing toxic levels of antimycin A²⁴. We also observed significantly higher L_N in the presence of AOX (**Figure 5A and B**), which results in a lower RCR (**Figure 5C**). This estimate of lower mitochondrial coupling indicates higher energy dissipation, which is again consistent with a thermogenic role for AOX in *Drosophila* larvae cultured at low temperatures. However, additional experiments are warranted to show how much heat AOX produces and how this changes metazoan mitochondrial metabolism. This may include investigations testing other mitochondrial electron transfer pathways and other temperatures. Notably, the Oroboros high resolution respirometry system is a versatile equipment, allowing different combination of protocols to test the mitochondrial electron transfer system in different ways. In addition, and perhaps more importantly, the protocols can be optimized as needed and the interested *Drosophilist* can count on a large online community of O2k users specialized in mitochondria of diverse tissues, and on the open-source materials provided by the company in their website⁴³.

ACKNOWLEDGMENTS:

We would like to thank Emily A. McKinney for English editing of the manuscript. G.S.G. was supported by a fellowship from the Conselho Nacional de Desenvolvimento Científico e Tecnológico (CNPq, grant number 141001/2019-4). M.T.O. would like to acknowledge funding from the Fundação de Amparo à Pesquisa do Estado de São Paulo (FAPESP, grant numbers 2014/02253-6 and 2017/04372-0), and the CNPq (grant numbers 424562/2018-9 and 306974/2017-7). C.A.C.-L. would like to acknowledge internal financial support from the Universidade do Oeste Paulista. The work with genetically modified *Drosophila* lines was authorized by the Local Biosafety Committee (CIBio) of the Faculdade de Ciências Agrárias e Veterinárias de Jaboticabal, under the protocols 001/2014 and 006/2014, and by the National Technical Committee on Biosafety (CTNBio), under the protocols 36343/2017/SEI-MCTIC, 01200.706019/2016-45, and 5488/2017.

DISCLOSURES:

The authors declare no conflict of interest.

REFERENCES:

1. <<https://www.nobelprize.org/prizes/medicine/>>.
2. <https://pubmed.ncbi.nlm.nih.gov/?term=%22drosophila+model%22&filter=datesearch.y_5>.

3. <<https://nexus.od.nih.gov/all/2016/07/14/a-look-at-trends-in-nihs-model-organism-research-support/>>.
4. <<https://bv.fapesp.br/pt/metapesquisa/?q=drosophila,>>.
5. <<https://bv.fapesp.br/pt/metapesquisa/>>.
6. Jennings, B.H. *Drosophila*-a versatile model in biology & medicine. *Materials Today*. **14** (5), 190–195, doi: 10.1016/S1369-7021(11)70113-4 (2011).
7. Brandt, A., Vilcinskas, A. The Fruit Fly *Drosophila melanogaster* as a Model for Aging Research. *Yellow Biotechnology I. Advances in Biochemical Engineering/Biotechnology*. **135**, 63–77, doi: 10.1007/10 (2013).
8. Yang, D. Simple homemade tools to handle fruit flies—*drosophila melanogaster*. *Journal of Visualized Experiments*. **2019** (149), 1–8, doi: 10.3791/59613 (2019).
9. Cheluvappa, R., Scowen, P., Eri, R. Ethics of animal research in human disease remediation, its institutional teaching; and alternatives to animal experimentation. *Pharmacology Research and Perspectives*. **5** (4), doi: 10.1002/prp2.332 (2017).
10. <http://www.planalto.gov.br/ccivil_03/_ato2007-2010/2008/lei/l11794.htm>.
11. <https://www.planalto.gov.br/ccivil_03/_ato2004-2006/2005/decreto/d5591.htm>.
12. <<https://revistapesquisa.fapesp.br/en/supply-side-research-constraints/>>.
13. <<http://www.abc.org.br/2014/05/08/em-depoimento-a-cell-dario-zamboni-fala-dos-desafios-de-produzir-boa-ciencia-no-brasil/>>.
14. Nascimento, S., Pólvara, A. Maker Cultures and the Prospects for Technological Action. *Science and Engineering Ethics*. **24** (3), 927–946, doi: 10.1007/s11948-016-9796-8 (2018).
15. Maia Chagas, A., Prieto-Godino, L.L., Arrenberg, A.B., Baden, T. The €100 lab: A 3D-printable open-source platform for fluorescence microscopy, optogenetics, and accurate temperature control during behaviour of zebrafish, *Drosophila*, and *Caenorhabditis elegans*. *PLoS Biology*. **15** (7), doi: 10.1371/journal.pbio.2002702 (2017).
16. Baden, T., Chagas, A.M., Gage, G., Marzullo, T., Prieto-Godino, L.L., Euler, T. Open Labware: 3-D Printing Your Own Lab Equipment. *PLOS Biology*. **13** (3), e1002086, doi: 10.1371/journal.pbio.1002086 (2015).
17. Zhou, B., Tian, R. Mitochondrial dysfunction in pathophysiology of heart failure. *Journal of Clinical Investigation*. **128** (9), 3716–3726, doi: 10.1172/JCI120849 (2018).
18. Hock, D.H., Robinson, D.R.L., Stroud, D.A. Blackout in the powerhouse: Clinical phenotypes associated with defects in the assembly of OXPHOS complexes and the mitoribosome. *Biochemical Journal*. **477** (21), 4085–4132, doi: 10.1042/BCJ20190767 (2020).
19. Juszczuk, I.M., Rychter, A.M. Alternative oxidase in higher plants. *Acta Biochimica Polonica*. **50** (4), 1257–1271, doi: 10.18388/abp.2003_3649 (2003).
20. McDonald, A.E. Alternative oxidase: An inter-kingdom perspective on the function and regulation of this broadly distributed “cyanide-resistant” terminal oxidase. *Functional Plant Biology*. **35** (7), 535–552, doi: 10.1071/FP08025 (2008).
21. McDonald, A.E., Vanlerberghe, G.C., Staples, J.F. Alternative oxidase in animals: Unique characteristics and taxonomic distribution. *Journal of Experimental Biology*. **212**, 2627–2634, doi: 10.1242/jeb.032151 (2009).
22. McDonald, A., Vanlerberghe, G. Branched Mitochondrial Electron Transport in the Animalia: Presence of Alternative Oxidase in Several Animal Phyla. *IUBMB Life (International Union of Biochemistry and Molecular Biology: Life)*. **56** (6), 333–341, doi: 10.1080/1521-

6540400000876 (2004).

23. McDonald, A.E., Costa, J.H., Nobre, T., De Melo, D.F., Arnholdt-Schmitt, B. Evolution of AOX genes across kingdoms and the challenge of classification. *Alternative Respiratory Pathways in Higher Plants*. (May), 267–272, doi: 10.1002/9781118789971.ch15 (2015).

24. Fernandez-Ayala, D.J.M. *et al.* Expression of the *Ciona intestinalis* Alternative Oxidase (AOX) in *Drosophila* Complements Defects in Mitochondrial Oxidative Phosphorylation. *Cell Metabolism*. **9** (5), 449–460, doi: 10.1016/j.cmet.2009.03.004 (2009).

25. Kemppainen, K.K. *et al.* Expression of alternative oxidase in *Drosophila* ameliorates diverse phenotypes due to cytochrome oxidase deficiency. *Human Molecular Genetics*. **23** (8), 2078–2093, doi: 10.1093/hmg/ddt601 (2014).

26. Andjeković, A., Kemppainen, K.K., Jacobs, H.T. Ligand-bound geneswitch causes developmental aberrations in *drosophila* that are alleviated by the alternative oxidase. *G3: Genes, Genomes, Genetics*. **6** (9), 2839–2846, doi: 10.1534/g3.116.030882 (2016).

27. Hakkaart, G.A.J., Dassa, E.P.E.P., Jacobs, H.T., Rustin, P. Allotopic expression of a mitochondrial alternative oxidase confers cyanide resistance to human cell respiration. *EMBO Reports*. **7** (3), 341–345, doi: 10.1038/sj.embor.7400601 (2006).

28. Dassa, E.P. *et al.* Expression of the alternative oxidase complements cytochrome c oxidase deficiency in human cells. *EMBO Molecular Medicine*. **1** (1), 30–36, doi: 10.1002/emmm.200900001 (2009).

29. Szibor, M. *et al.* Broad AOX expression in a genetically tractable mouse model does not disturb normal physiology. *DMM Disease Models and Mechanisms*. **10** (2), 163–171, doi: 10.1242/dmm.027839 (2017).

30. El-Khoury, R., Kaulio, E., Lassila, K.A., Crowther, D.C., Jacobs, H.T., Rustin, P. Expression of the alternative oxidase mitigates beta-amyloid production and toxicity in model systems. *Free Radical Biology and Medicine*. **96**, 57–66, doi: 10.1016/j.freeradbiomed.2016.04.006 (2016).

31. Mills, E.L. *et al.* Succinate Dehydrogenase Supports Metabolic Repurposing of Mitochondria to Drive Inflammatory Macrophages. *Cell*. **167** (2), 457–470.e13, doi: 10.1016/j.cell.2016.08.064 (2016).

32. Giordano, L. *et al.* Alternative Oxidase Attenuates Cigarette Smoke-induced Lung Dysfunction and Tissue Damage. *American Journal of Respiratory Cell and Molecular Biology*. **60** (5), 515–522, doi: 10.1165/rcmb.2018-0261OC (2019).

33. Camargo, A.F. *et al.* Xenotopic expression of alternative electron transport enzymes in animal mitochondria and their impact in health and disease. *Cell biology international*. **42** (6), 664–669, doi: 10.1002/cbin.10943 (2018).

34. Saari, S. *et al.* Alternative respiratory chain enzymes: Therapeutic potential and possible pitfalls. *Biochimica et Biophysica Acta - Molecular Basis of Disease*. **1865** (4), 854–866, doi: 10.1016/j.bbadis.2018.10.012 (2019).

35. <<https://www.instructables.com/Building-a-Prusa-I3-3D-Printer-Revisited/>>.

36. <<https://www.tinkercad.com/>>.

37. <<https://www.repetier.com/>>.

38. <<https://www.tinkercad.com/login>>.

39. <<https://knowledge.autodesk.com/support/revit-products/learn-explore/caas/CloudHelp/cloudhelp/2016/ENU/Revit-Model/files/GUID-B89AD692-C705-458F-A638-EE7DD83D694C-htm.html>>.

- 925 40. Koemans, T.S. *et al.* Drosophila courtship conditioning as a measure of learning and
926 memory. *Journal of Visualized Experiments*. **2017** (124), 55808, doi: 10.3791/55808 (2017).
- 927 41. Ali, Y.O., Escala, W., Ruan, K., Zhai, R.G. Assaying locomotor, learning, and memory deficits
928 in Drosophila models of neurodegeneration. *Journal of Visualized Experiments*. (49), doi:
929 10.3791/2504 (2011).
- 930 42. Nichols, C.D., Becnel, J., Pandey, U.B. Methods to assay Drosophila behavior. *Journal of*
931 *visualized experiments : JoVE*. **61** (e3795), doi: 10.3791/3795 (2012).
- 932 43. <<https://www.orooboros.at/>>.
- 933 44. Bradford, M.M. A rapid and sensitive method for the quantitation of microgram quantities
934 of protein utilizing the principle of protein-dye binding. *Analytical Biochemistry*. **72** (1–2), 248–
935 254, doi: 10.1016/0003-2697(76)90527-3 (1976).
- 936 45. <<https://tinkercad.zendesk.com/hc/en-us/categories/200357447-FAQ>>.
- 937 46. Morton, J.D., Barnes, M.F., Zyskowski, R.F. Respiratory control ratio: A computer
938 simulation of oxidative phosphorylation. *Biochemical Education*. **24** (2), 110–111, doi:
939 10.1016/0307-4412(95)00156-5 (1996).
- 940 47. Chance, B., Williams, G.R. Respiratory enzymes in oxidative phosphorylation. I. Kinetics of
941 oxygen utilization. *The Journal of Biological Chemistry*. **217** (1), 383–393, at
942 <<https://pubmed.ncbi.nlm.nih.gov/13271402/>> (1955).
- 943 48. Geissmann, Q., Garcia Rodriguez, L., Beckwith, E.J., French, A.S., Jamasb, A.R., Gilestro,
944 G.F. Ethoscopes: An open platform for high-throughput ethomics. *PLOS Biology*. **15** (10),
945 e2003026, doi: 10.1371/journal.pbio.2003026 (2017).
- 946 49. <<https://github.com/amchagas/Flypi>>.
- 947 50. <<https://gilestrolab.github.io/ethoscope/>>.
- 948 51. <<https://imagej.nih.gov/ij/>>.
- 949 52. <<https://open-neuroscience.com/>>.
- 950 53. <https://www.appropedia.org/3D_printable_science_equipment>.
- 951 54. McParland, A.L., Follansbee, T.L., Ganter, G.K. Measurement of larval activity in the
952 Drosophila activity monitor. *Journal of Visualized Experiments*. doi: 10.3791/52684 (2015).
- 953 55. Schou, M.F., Kristensen, T.N., Pedersen, A., Göran Karlsson, B., Loeschcke, V., Malmendal,
954 A. Metabolic and functional characterization of effects of developmental temperature in
955 Drosophila melanogaster. *American Journal of Physiology - Regulatory Integrative and*
956 *Comparative Physiology*. **312** (2), R211–R222, doi: 10.1152/ajpregu.00268.2016 (2017).
- 957 56. Meeuse, B.J.D. Thermogenic Respiration in Aroids. *Annual Review of Plant Physiology*. doi:
958 10.1146/annurev.pp.26.060175.001001 (1975).
- 959 57. Watling, J.R., Robinson, S.A., Seymour, R.S. Contribution of the alternative pathway to
960 respiration during thermogenesis in flowers of the sacred lotus. *Plant Physiology*. doi:
961 10.1104/pp.105.075523 (2006).
- 962 58. Inaba, Y.I. *et al.* Alternative oxidase capacity of mitochondria in microsporophylls may
963 function in cycad thermogenesis. *Plant Physiology*. **180** (2), 743–756, doi: 10.1104/pp.19.00150
964 (2019).
- 965 59. Sanz, A., Stefanatos, R., McIlroy, G. Production of reactive oxygen species by the
966 mitochondrial electron transport chain in Drosophila melanogaster. *Journal of Bioenergetics and*
967 *Biomembranes*. **42** (2), 135–142, doi: 10.1007/s10863-010-9281-z (2010).
- 968 60. Miwa, S., St-Pierre, J., Partridge, L., Brand, M.D. Superoxide and hydrogen peroxide

969 production by Drosophila mitochondria. *Free Radical Biology and Medicine*. **35** (8), 938–948, doi:
970 10.1016/S0891-5849(03)00464-7 (2003).

971 61. Gnaiger, E. *Mitochondrial Pathways and Respiratory Control An Introduction to OXPHOS*
972 *Analysis. Bioenergetics Communications*. **2**, doi: 10.26124/bec:2020-0002. Bionergetics
973 Communications. Innsbruck, Austria. (2020).

974

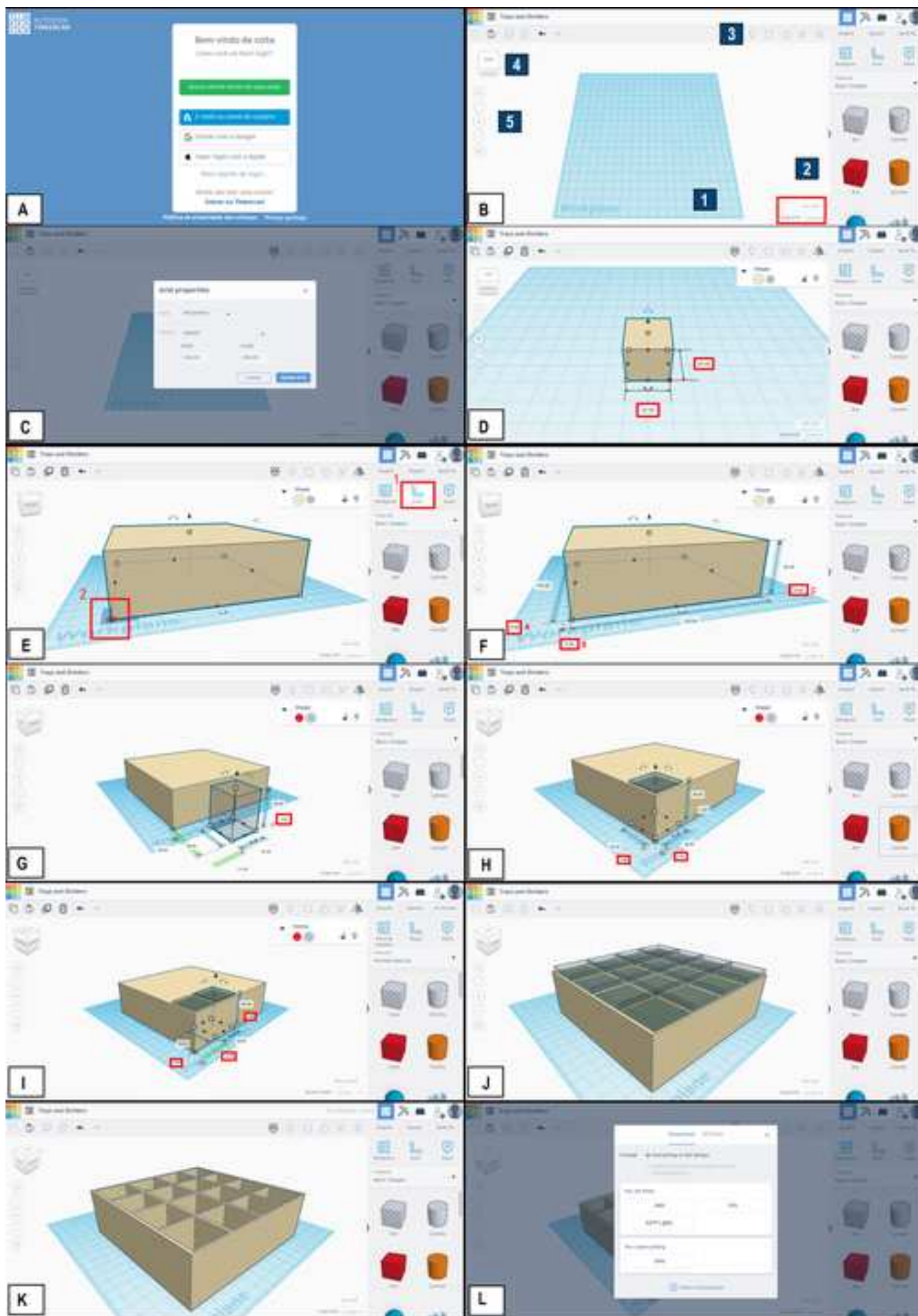


Figure 2

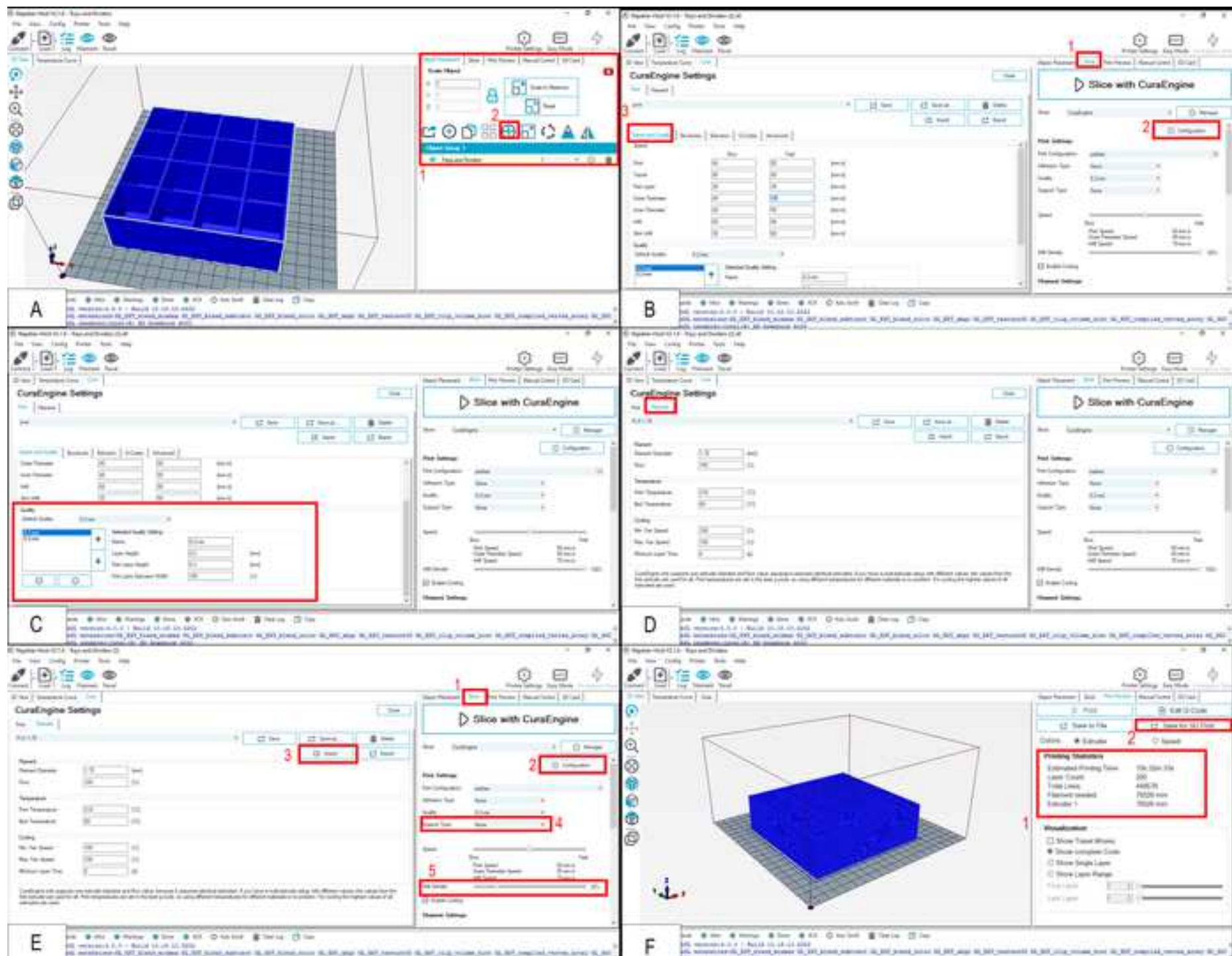
[Click here to access/download;Figure;Figure 2 new.tif](#)

Figure 3

[Click here to access/download;Figure;Figure 3.tif](#)

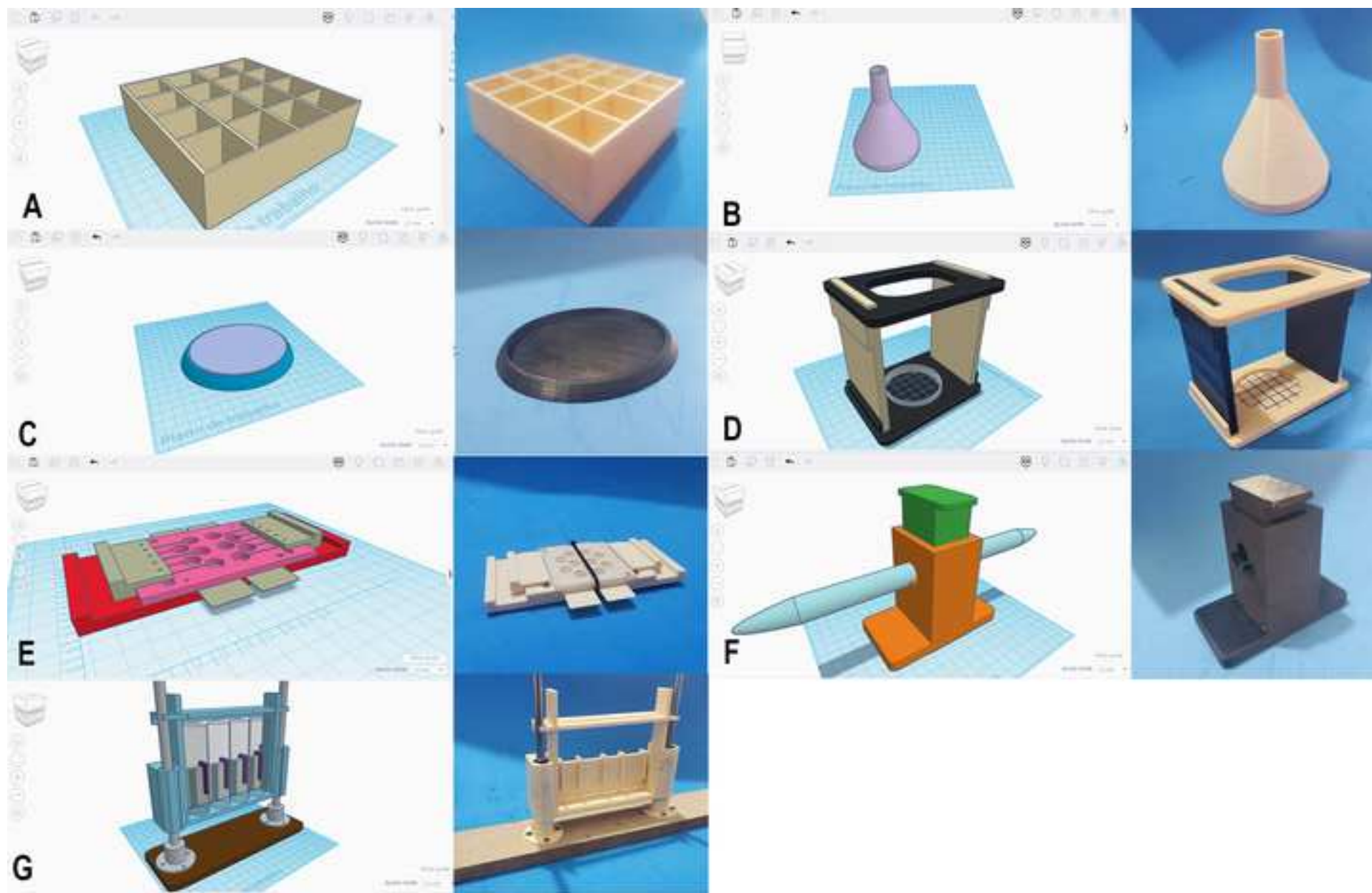
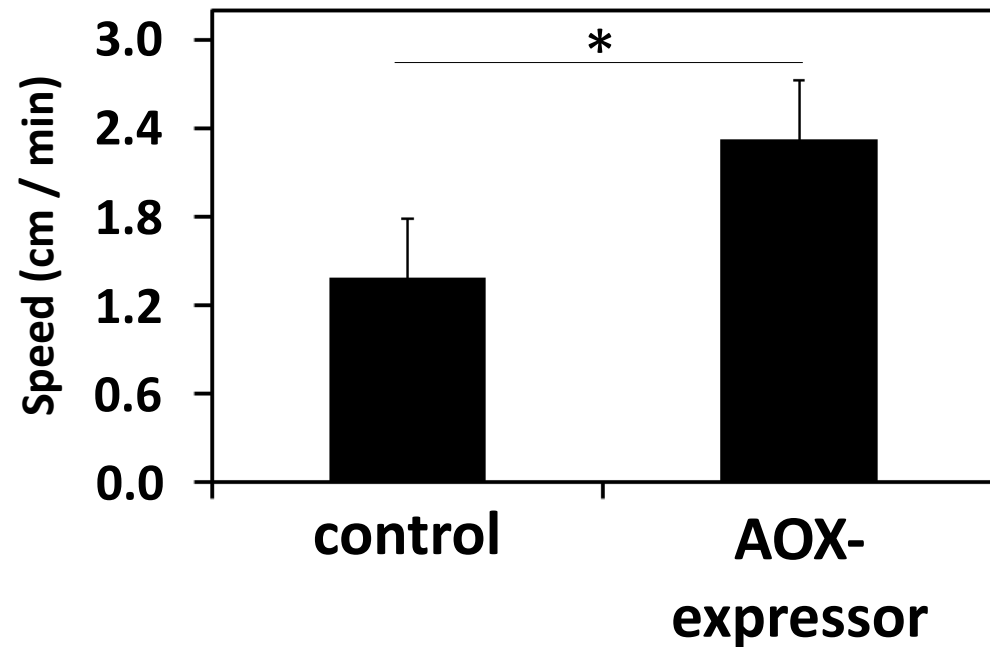
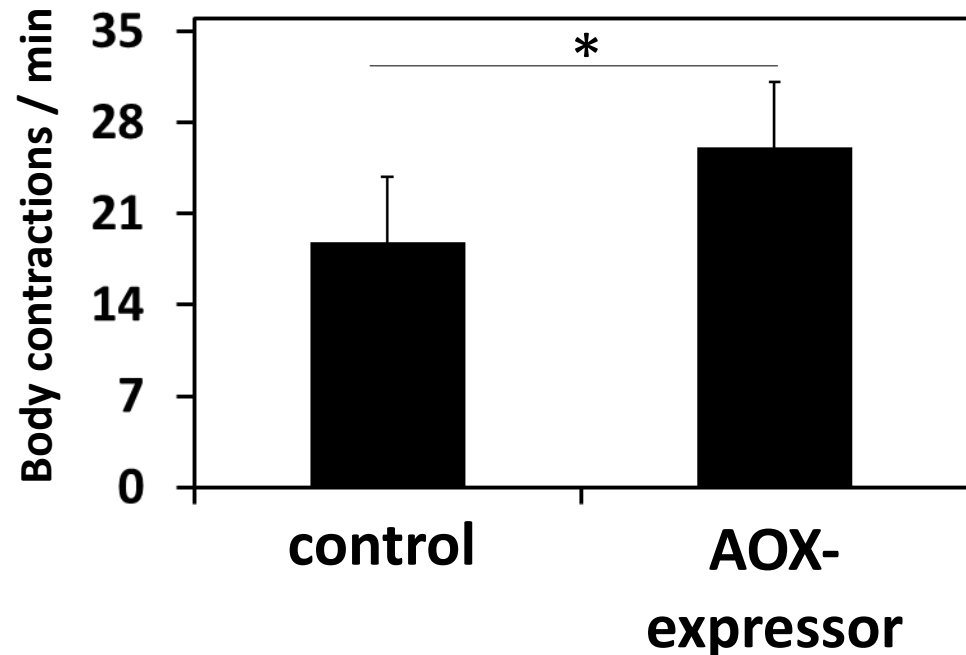


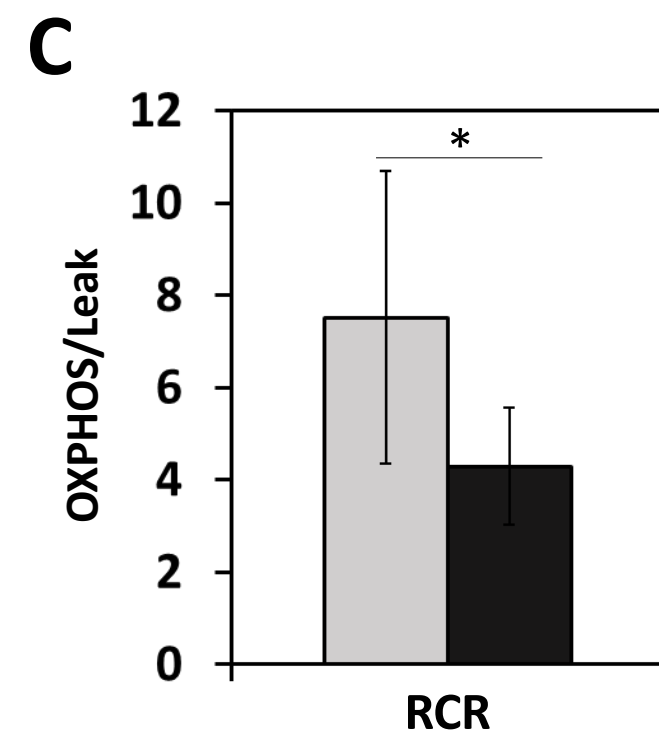
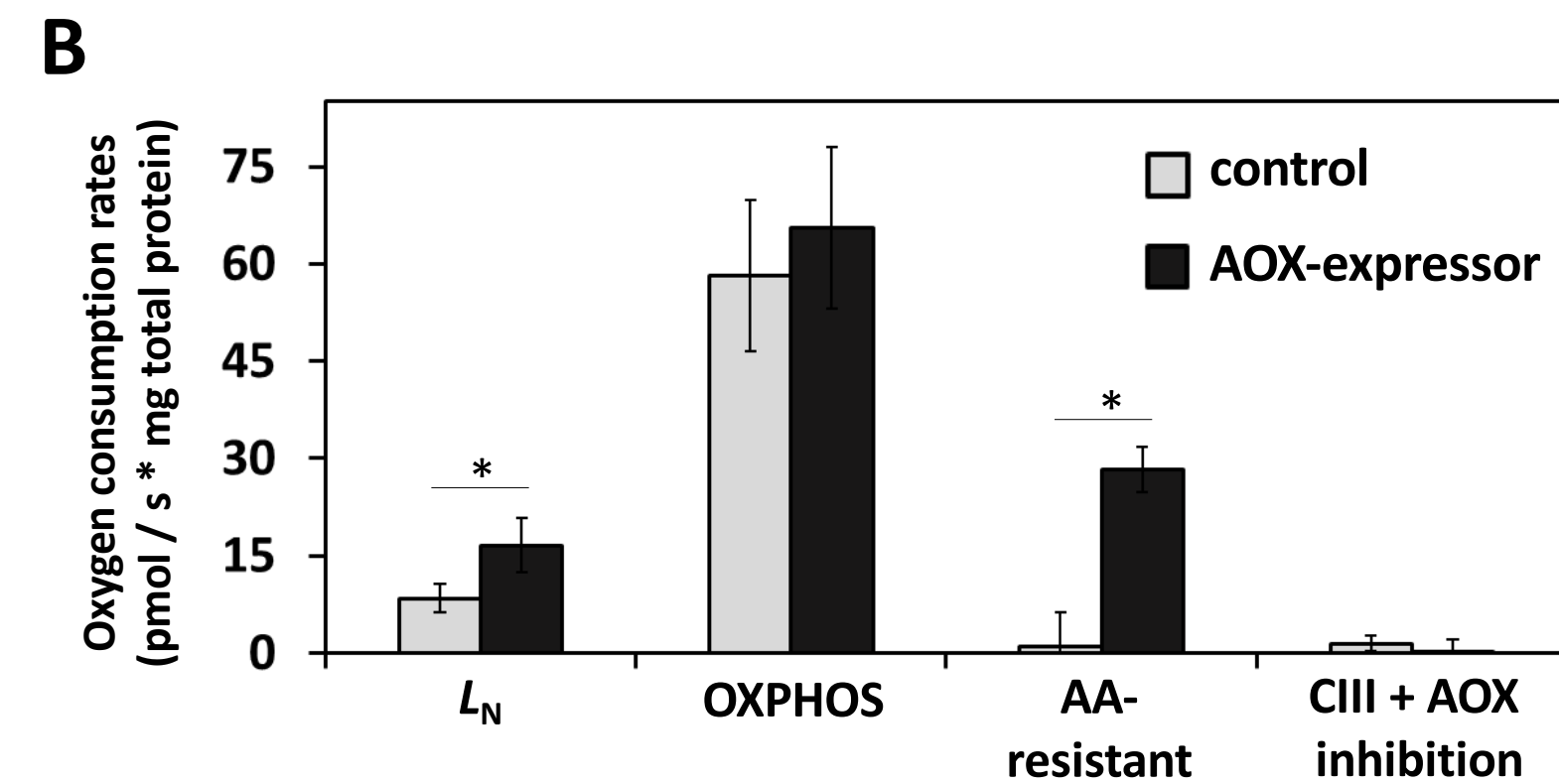
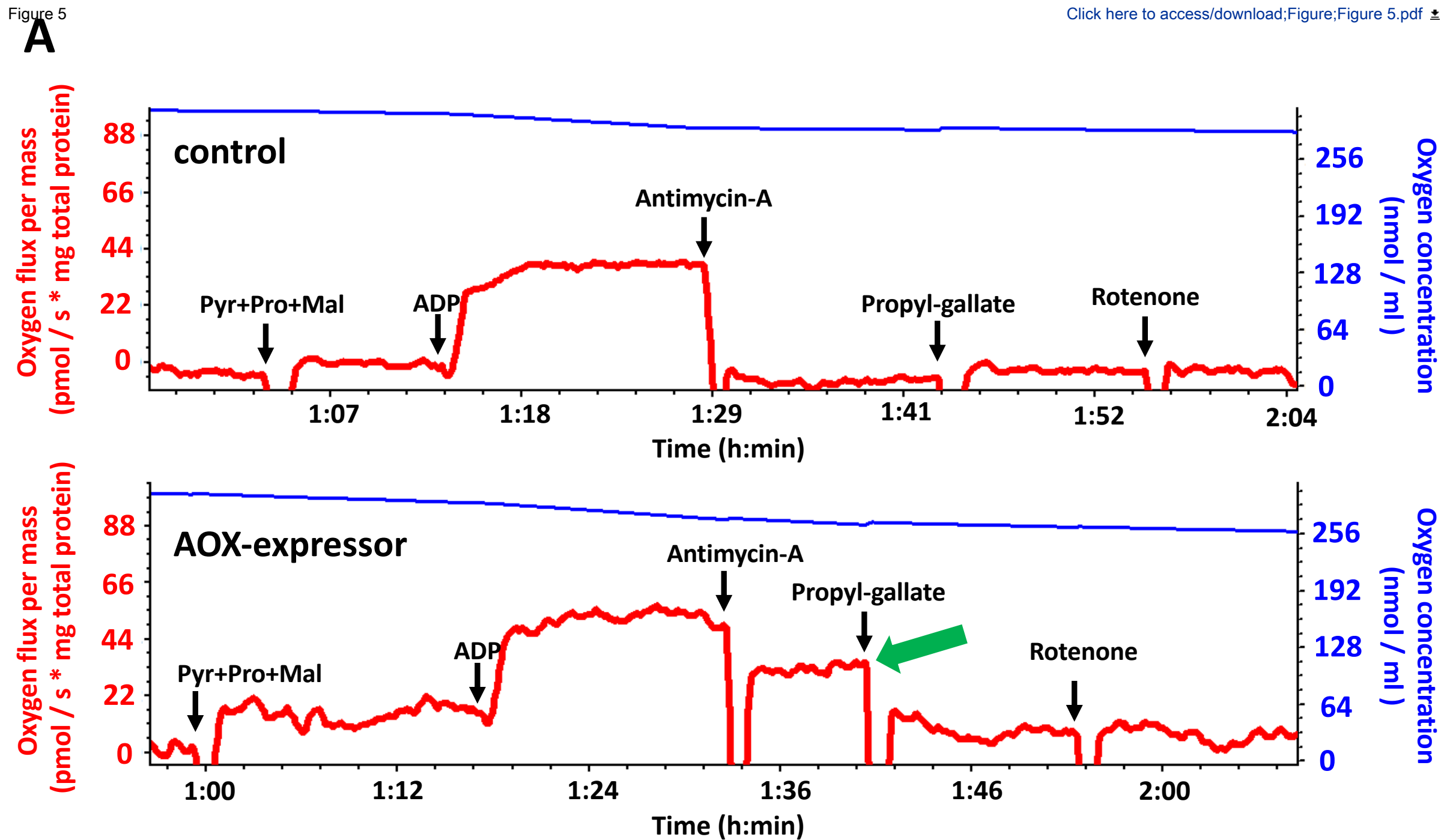
Figure 4

A



B







Click here to access/download
Table of Materials
Table of Materials1.xlsx

Response to the editorial and reviewers' comments
Garcia et al., manuscript ID JoVE62669

We would like to thank all people involved in the scientific and editorial review of our manuscript, especially for the patience as we faced critical moments of the current COVID-19 pandemic during the writing and revision of the work. We have revamped our manuscript along the lines proposed by the reviewers. In the new version, we indicate changes introduced in response to criticisms in red text, with accompanying marginal red boxes numbered according to specific reviewer or editorial comments, as below. We also would like to state that the revision of our manuscript required the intense participation of another member of our lab, Murilo F. Othonicar, whose name has now been removed from the Acknowledgements, and added as a coauthor in this work. We hope our manuscript is now suitable for publication in JoVE.

Editorial and production comments:

E1. Please take this opportunity to thoroughly proofread the manuscript to ensure that there are no spelling or grammar issues.

We believe we have proofread all document after revision, and that it should be ready for publication after the reviewers' reevaluation. We have also included a new author in the manuscript.

E2. Please revise the title for conciseness.

The title is now under JoVE's guidelines of no more than 150 characters: An affordable and efficient "homemade" platform for *Drosophila* behavioral studies, and an accompanying protocol for larval mitochondrial respirometry

E3. Please do not provide URLs in the article text. You can cite these URLs as superscripted numbers similar to the references.

URLs have been moved to the reference list and are now cited with superscripted numbers in the main text.

E4. The Protocol should contain only action items that direct the reader to do something. Please move the discussion about the protocol to the Discussion.

We believe we have moved everything that is not essential for the protocol to the discussion section. We have, however, left the introductory paragraph of each protocol, as we consider this essential to contextualize the reader.

E5. Please ensure that all text in the protocol section is written in the imperative tense as if telling someone how to do the technique (e.g., "Do this," "Ensure that," etc.). The actions should be described in the imperative tense in complete sentences wherever possible.

We have revised the Protocols section accordingly, and believe it now meets the requirements described here, except perhaps for Protocol 3. This protocol has a distinct nature, so we consider that its current format is very informative to the reader and that should not be altered.

Reviewers' comments:

Reviewer #1:

Manuscript Summary:

This manuscript aims to introduce the use of 3D printing in drosophila research and provides examples of the types of equipment that can be produced. Further it shows how some of the equipment can be used to perform physiology studies on the flies.

We appreciate the comprehensive review provided by reviewer #1. We have edited the manuscript to address every single comment below to the best of our abilities. The 3D design and printing protocols have been improved significantly.

R1.1: My biggest concern is that while I wholeheartedly support the use and expanded use of 3D printing in all types of research, and agree that it can democratize access to equipment and research opportunities, this particular manuscript seems to fall in between the cracks. Its not enough of a guide in terms of the specifics needed for a complete novice that has never done any 3D printing or drosophila work so I worry that it will leave readers confused or not feeling capable of carrying out the presented work, and at the same time for those that do know how to do this and just need the files, all but the respirometry protocols are unnecessary.

In this revised version of the manuscript, we have significantly increased the details in Protocols 1 (3D model design) and 2 (3D printing), and Figures 1 and 2, in order to provide the reader enough guidance in conducting the design and printing of a fly vial rack. We realize that, even after these changes, the protocols might still be challenging for first time users, so we have included a sentence in the beginning of the Protocols and of the Results sections emphasizing that the 3D printing beginners should get acquainted with the different software and their help centers to ensure proper results. We are also counting on the video to provide the reader a more complete guide to the procedures.

R1.2: Making the files available on a common site like Thingiverse would handle the latter, and a lot more would be needed to support the former. That said, if this allows researchers that would otherwise not be thinking of this route to find out about this (and that's not something I convinced will happen), its great. I just wonder if a whole JOVE video is warranted without more basic "how-

to" and explanations of terms etc...(e.g. infill, supports, slicing etc...). Maybe that would be in the final video, it's hard for me to tell.

Please, see response to comment R1.1 above. In addition, we do agree with the reviewer that making our STL files available via Thingiverse would ultimately provide what more advanced 3D printing Drosophilist users need. However, we believe that there is no better way to disseminate scientific content than by providing our files via a thoroughly peer-reviewed scientific publication. Although not infallible, good peer review is the gold standard of science, so we believe the researcher audience we are aiming at will be more trustful if our files are available through the JoVE website.

R1.3) I still do not see where the authors come to the conclusion that its this misunderstanding that is holding back drosophila research. It may be, but it seems like its an unsubstiated guess. I would at least like to see them base it on pers. comm, or other first hand experience if they cannot point to studies or other empirical data.

The reviewer is right that this is pure speculation. To the best of our knowledge, there are no hard data on the matter, but we are planning on conducting an investigation in the future to provide reliable numbers to substantiate our statements. Meanwhile, for the purpose of this manuscript, we rewrote the referred passage of the text to clarify that this is indeed a speculation and that the issue of Drosophila research **in Brazil** being held back might **also** be due to the high costs of importing equipment, which is inherent to any scientific research area in the country. To circumvent the high costs and need for imports, we offer 3D printing protocols for new and established Drosophila researchers.

R1.4) What GMO are they referring to that would be a replacement for Dros.? Seems like a strawman and unnecessary.

We apologize for the confusion. Working with GMOs in Brazil requires authorizations, which can take time to be granted due to bureaucracy (please, see details in the response to comment R1.6), and is therefore a negative aspect of the work, considering that basically all work with Drosophila models of human biology/disease involve the use of transgenic lines. We have now clarified our statement in the manuscript.

R1.5) Could the authors approximate the cost of non-printed equipment to give the reader a feel for the limitation level? Is access to the 3D printing tech cheaper and easier to get (i.e. not imported etc...)

This is a matter of demand and supply. Even though a personal 3D printer is also an imported piece of equipment, it can be purchased in any tech website for anyone in the country to use in a variety of domestic needs (our latest acquisition costed ~R\$1,900.00 – i.e., ~US\$380.00), whereas specialized fly apparatuses are only needed by few lab researchers, aiming at conducting behavioral or other analyses. How reduced the costs of printing and assembling homemade lab

equipment are is classically represented by the FlyPi, which can be built for less than €100.00 and serves as a light and fluorescence microscope able to use opto- and thermogenetic stimulation of the genetically tractable zebrafish, *Drosophila* and nematodes. We have recently received a quote of a basic Zeiss fluorescence microscope for the price of €41,449.11, an amount of money sufficient to pay the salary of two PhD students (or one post-doc) for 4 years. We provide the quote attached to this rebuttal letter and apologize it is only in Portuguese. However, the equipment specifications are easily translatable even without basic knowledge of the language, and the price is clearly shown. To illustrate to the reader of our manuscript how cheap printed equipment can be, we have now included the example of the FlyPi in the introduction.

R1.6) Out of curiosity, since you are using a transgene for the OXPHOS work, does that need permission, or is any fly work is exempt? (since you bring it up earlier).

According to the Brazilian law, all work with GMOs must be authorized by an expert committee, after an evaluation that will determine environmental, animal and human health safety. In the case of GM *Drosophila*, the Local Biosafety Committee of each institution can provide such authorization, given that the National Technical Committee on Biosafety has previously approved the use of particular lab spaces for activities with GMOs. Work with non-GM flies does not require a biosafety authorization. We have now included our authorization numbers in the Acknowledgements section.

R1.7) Line 162: worth noting that access is free with a simple registration

The information has been included.

R1.8) Line 167-: if you are going to go into this amount of detail, do you need to provide info on how to move, align the boxes? i.e., click and drag, and setting the movement scale (i.e. to mm or 0.1mm etc...)?

As part of the response to the reviewer's comment R1.1 (see above), we have included more procedural details in Protocol 1, especially in the new steps 1.6 and 1.7, which should also address this comment sufficiently.

R1.9) If this is really to be an intro to 3D printing, which it appears to be (for people that have done this before) an explanation of what infill or supports are and when they are necessary or not seems to be in order. The use of 100% infill seems unnecessary, just adding to time, materials used and chances of things going wrong. If this is needed, please explain why.

We thank the reviewer for pointing out our mistake. We corrected the manuscript to say "20% infill", as this is standard for our 3D printed pieces. We have also included explanations about infill, supports and other printing parameters in the Discussion section and in the legend to Figure 2.

R1.10) *Line 255-270 I do not think the way "modular" is being used is correct.*

We have excluded this term from steps 3.4 and 3.5 of Protocol 3.

R1.11) *Line 460: I think this is sort of an overstatement in terms of what this manuscript provides.*

Although we have improved Protocols 1 and 2 substantially, we have also rewritten the beginning of the Results section, the Abstract, the Summary and the Introduction to ensure this comment of the reviewer is properly addressed, and that we are not giving the reader the false impression that we are providing solutions for all lab problems with our protocols.

Reviewer #2:

Manuscript Summary:

The manuscript aims to describe simple and affordable protocols for rearing and behavioral studies in Drosophila melanogaster. Secondly, this manuscript describes methods for measuring mitochondrial respiration in Drosophila larvae. Mutant Drosophila strains are used to assess the role of mitochondrial alternative oxidase on larval locomotion and mitochondrial respiration. Overall, this manuscript is well written and very thorough.

The AOX portion of this manuscript is very interesting. I look forward to seeing this work continue in the future.

We truly appreciate the positive comments, and can assure more interesting work using AOX-expressing flies will be available in the near future.

R2.1) *There are some grammatical and type-editing that needs to be done.*

We ourselves have revised the manuscript thoroughly for these errors, and the manuscript has gone through professional scientific English revision, so we hope everything is fixed now.

Reviewer #3:

Manuscript Summary:

The authors described in detail the methods of 3D-printing various instruments used in fly behavior experiments and the method of measuring oxygen consumption in the mitochondria of fruit fly larvae. The article describes step-by-step steps how to use 3D model design software to design models, 3D-printing, at the same time, considering that it is very time-consuming for beginners to use 3D modeling software to design models from beginning, the authors generously provided readers with several designed models files they created for downloading.

The method described in this article is not only suitable for developing countries where materials are relatively scarce, even the simplest experimental instruments (such as funnels) need to be imported, but also suitable for developing countries or developed countries with relatively better economic conditions and relatively abundant resources, as even in these countries, not all research groups have sufficient funds to afford expensive instruments. In addition, the instruments provided by biotechnology companies are not always suitable for the needs of researchers. Researchers sometimes need to improve existing experimental instruments or design and manufacture instruments suitable for their own experiments. The 3D printing described in the article is a better choice.

We are glad to hear the reviewer foresee our protocols being useful in labs in developing and developed countries alike.

R3.1) *It is advisable to use the symbol Φ to indicate the diameter, such as line 294, "90 X 15 mm Petri dishes". Although there are such expressions in the literature, I think it is more reasonable to use $\Phi 90 \times 15$ mm.*

We have included the symbol Φ in every instance needed to indicate diameter measurements.

Fund Amparo a Pesq doEst de S Paulo
Departamento de Tecnologia, FCAV/UNESP
Dr. Marcos Túlio de Oliveira
R Pio XI 1500
Alto da Lapa
SAO PAULO - SP
05468-901
BRASIL

Carl Zeiss do Brazil Ltda.
Rod Antonio Heil 1001 KM01
Armz G11 Itajaí,SC
88316-001
Brasil

Contato Comercial

Nome: Loiola João
Telefone:
Fax:
E-mail: joao.loiola@neomeddobrasil.com.br

Data: 20/05/2021
Página: 1 de 5

Proposta

Proposta N°: 7760692220

Cliente N°: 10892

Na qualidade de representante exclusivo no Brasil, da empresa Carl Zeiss Alemanha, temos o prazer de oferecer:

Item	Descrição do Produto	Quant.
10	Microscopio Axioscope 5/7 KMAT Consisting of the following items:	1 PC
20	Microscope stand Axioscope 5, TL/FL,	1 PC
30	Tubo trinocular com saída para camera	1 PC
40	Ocular PL 10x/23 Br. foc.	2 PC
50	Protetor para ocular	2 PC
60	Suporte para protecao ocular	1 PC
70	Luneta para alinhamento de aneis de fase	1 PC
80	Sistema de iluminacao Colibri 3, UV / B	1 PC
90	Platina Mecanica 75X50 R	1 PC
100	Suporte para Lamina 76X26 Mm	1 PC
110	Suporte para Platina D/A	1 PC
120	Slider de bloqueio A 14x40 mm	1 PC
130	Filtro de balanço de branco , d=32x1.5	1 PC
140	Filtro verde para banda de interferencia	1 PC
150	Filtro Azul D= 32X2 mm	1 PC



160	Filtro conversor 5700-3200 K, d=32 mm	1 PC
170	Jogo de filtro 50 incluso modulo	1 PC
180	Jogo de filtro 38 HE incluso modulo	1 PC
190	Jogo de filtro 43 HE incluso modulo	1 PC
200	Jogo de filtro 96 HE incluso modulo	1 PC
210	Reflector Turret 6x cod	1 PC
220	Suporte para Condensador c/Aju	1 PC
230	Condensador 0.9/1.25 H para objetivas de	1 PC
240	Disco Modulador H, D 0.65, Contraste de	1 PC
250	Polarizacao - Polarizador D, 90#	1 PC
260	Modulo Analizador Pol Acr P&C	1 PC
270	Objetiva N-Achroplan 5x/0.15 Ph1	1 PC
280	Objetiva N-Achroplan 10x/0.25 Ph1	1 PC
290	Objetiva N-Achroplan 20x/0.45 Ph2	1 PC
300	Objetiva N-Achroplan 63x/0.85 Ph3	1 PC
310	Objetiva EC Plan-Neofluar 40x/0.75 Ph2	1 PC
320	Objetiva EC Plan-Neofluar 100x/1.30 Oil	1 PC
330	Axiocam 705 mono	1 PC
340	Adaptador de camera 60N-C 1" 1.0x	1 PC
350	Adaptador duplo 60N - 2x 60N	1 PC
360	Espelho com divisor 100%	1 PC
370	SWR ZEN 3.3 pro DVD	1 PC
380	Conector de WiFi USB para ZEN	1 PC
390	Software DVD90 ZEN CORE 3.2	1 PC
400	Software DVD89 ZEN3.3 BLUE	1 PC
410	Adesivo fluorescente	1 PC
420	Adesivos para Axioimager	1 PC
430	Cover glassess 1,5 H, high-performance,	3 PC
440	oleo Imersao Immersol 518 FL 20ml	1 PC
450	Safety data sheet 40-809 F	1 PC
460	Caixa p/ 6 Pc Modulo Refletor	1 PC
470	Cabo BR/3-H05VV-F3G1.00-C13/2.5 bk	1 PC
480	Adaptador de camera 60N-C 2/3" 0.5x	1 PC
490	Axiocam 208 color	1 PC



Proposta Nº:	7760692220
Data:	20/05/2021
Página:	3 de 5

Subtotal	41.449,11 EUR
TOTAL	41.449,11 EUR

De acordo com os regulamentos de controle de exportação aplicáveis, incluindo as disposições do direito europeu e dos Estados Unidos da América em matéria de controle de exportação, esta cotação só entrará em vigor no caso de um embargo, se esse embargo for removido, ou, caso uma venda esteja sujeita a uma licença, só será efetiva se forem concedidas todas as licenças oficiais necessárias. Se o acordo não entrar em vigor com base nos regulamentos de controle de exportação aplicáveis, deve-se excluir qualquer reclamação contra a nossa parte, especialmente reclamações por danos.



Proposta N°:	7760692220
Data:	20/05/2021
Página:	4 de 5

Informações complementares:

Classificação fiscal sugerida (NCM - microscópio): 9011.80.20

Classificação fiscal sugerida (NCM - câmera): 8525.80.29

Aeroporto de Embarque: Frankfurt - Alemanha

Aeroporto de Embarque: Shanghai Pudong Airport (apagar caso o equipamento não venha da China)

Embalagem: Caixa de isopor revestida de papelão

"Frete Aéreo a pagar no destino (Collect) – Por Carga Aérea – Aeroporto de Guarulhos – São Paulo

CONDIÇÕES COMERCIAIS:

Validade da proposta: 60 (sessenta) dias a partir da data de emissão.

Prazo de fabricação: 150 (cento e cinquenta) dias a partir do recebimento do pedido oficial.

(Material embalado e disponibilizado para coleta na fábrica ou envio ao agente embarcador de acordo com o incoterm negociado).

Pagamento: CAD 21 dias

Dados do Fabricante:

Carl Zeiss (Suzhou) Ltd., Co.

Modern Industrial Square 3-B-2

No. 333, Xing Pu Road

ZIP CODE: 215126

Suzhou City, SIP - Jiangsu Province

Dados do Exportador:

CARL ZEISS MICROSCOPY GMBH

Promenade 10

D-07745 - Jena - Germany

Dados bancários do exportador:

Deutsche Bank AG

SWIFT/BIC: DEUTDE8EXXX

Account/IBAN: DE37 8207 0000 0620 0000 00

Quaisquer despesas bancárias legais ou de outra forma decorrentes do fornecimento e da transferência do respectivo pagamento são de responsabilidade do cliente.

A Carl Zeiss do Brasil Ltda, inscrita no CNPJ N.º 33.131.079/0001-49, estabelecida na Avenida das Nações Unidas, 12.495 - 9º andar - Cidade Monções - 04578-000 - São Paulo / SP, é representante exclusiva da Carl Zeiss Alemanha para todo o Brasil, fazendo jus a comissão de 15% sobre o valor total da proforma. Informamos que esta comissão não deverá ser retida no Brasil e que o cliente deverá remeter ao exterior o valor total da proforma.

GARANTIA:

De 12 (doze) meses a contar da instalação ou 15 meses a contar da liberação para o embarque, o que ocorrer primeiro contra defeitos de fabricação, excetuando-se artigos considerados de consumo.

Após o período de garantia, será oferecido um Contrato de Manutenção a ser executado pelo Departamento de Assistência Técnica da Carl Zeiss do Brasil, por técnicos especializados em todos os equipamentos ofertados.

INSTALAÇÃO:

A embalagem do produto apenas poderá ser aberta na presença de um profissional da Carl Zeiss do Brasil Ltda.



Proposta N°:	7760692220
Data:	20/05/2021
Página:	5 de 5

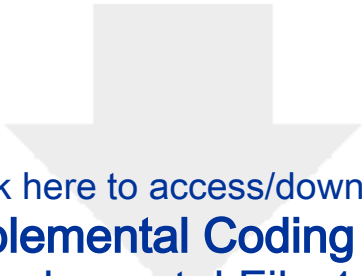
Após a entrega do equipamento, o cliente deverá entrar em contato com a Carl Zeiss do Brasil através do e-mail: relacionamento@zeiss.com para agendamento da instalação e/ou treinamento.

Os preços aqui consignados são os correntes no mercado de exportação para qualquer país. Não são publicadas listas de preços.


AS IMAGENS IMPRESSAS NA PROPOSTA SÃO MERAMENTE ILUSTRATIVAS E PODEM SER DIFERENTES DOS PRODUTOS ORIGINAIS.

Atenciosamente,
CARL ZEISS DO BRASIL LTDA.

João Victor Alves Loiola
Departamento Comercial
Divisão de Microscopia
NEOMED do Brasil
Estrada CIA Aeroporto, KM 12, Centro Emp. Aeroporto
Galpão 07
São Cristóvão - Salvador - BA
Tel./Phone.: + 55-71 - 2137-7093
Cel./Mobile.: + 55-71- 9 9199-5310
SAC: 0800 770 5556
joao.loiola@neomeddobrasil.com.br
www.neomeddobrasil.com.br




Click here to access/download
Supplemental Coding Files
Supplemental File 1.rcp





Click here to access/download
Supplemental Coding Files
Supplemental File 2.stl





Click here to access/download
Supplemental Coding Files
Supplemental File 3.stl






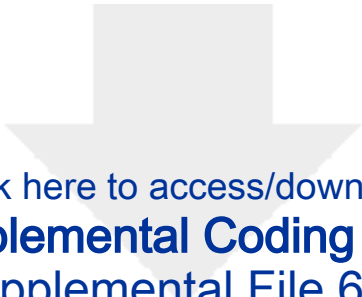
Click here to access/download
Supplemental Coding Files
Supplemental File 4.stl



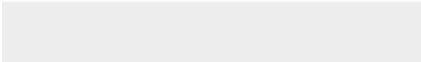


Click here to access/download
Supplemental Coding Files
Supplemental File 5.stl





Click here to access/download
Supplemental Coding Files
Supplemental File 6.stl



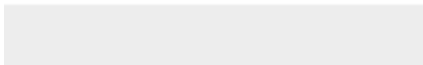


[Click here to access/download](#)
Supplemental Coding Files
Supplemental File 7.mp4



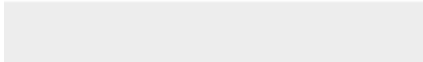


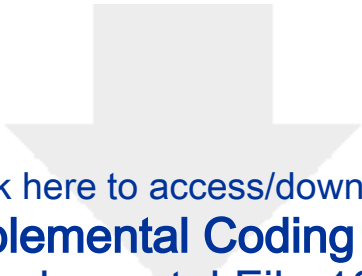
Click here to access/download
Supplemental Coding Files
Supplemental File 8.stl



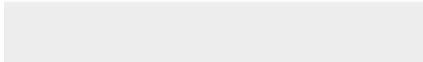



Click here to access/download
Supplemental Coding Files
Supplemental File 9.stl





Click here to access/download
Supplemental Coding Files
Supplemental File 10.stl





[Click here to access/download](#)
Supplemental Coding Files
Supplemental File 11.mp4

